

This is an Open Access document downloaded from ORCA, Cardiff University's institutional repository: <https://orca.cardiff.ac.uk/id/eprint/134809/>

This is the author's version of a work that was submitted to / accepted for publication.

Citation for final published version:

Tikani, Hamid, Setak, Mostafa and Demir, Emrah 2021. Multi-objective periodic cash transportation problem with path dissimilarity and arrival time variation. *Expert Systems with Applications* 164 , 114015. 10.1016/j.eswa.2020.114015

Publishers page: <https://doi.org/10.1016/j.eswa.2020.114015>

Please note:

Changes made as a result of publishing processes such as copy-editing, formatting and page numbers may not be reflected in this version. For the definitive version of this publication, please refer to the published source. You are advised to consult the publisher's version if you wish to cite this paper.

This version is being made available in accordance with publisher policies. See <http://orca.cf.ac.uk/policies.html> for usage policies. Copyright and moral rights for publications made available in ORCA are retained by the copyright holders.



Multi-objective periodic cash transportation problem with path dissimilarity and arrival time variation

Hamid Tikani¹, Mostafa Setak¹, Emrah Demir²

1. Department of Industrial Engineering, K. N. Toosi University of Technology, Tehran, Iran

2. PARC Institute of Manufacturing, Logistics and Inventory, Cardiff Business School, Cardiff University, Cardiff, United Kingdom

Abstract:

This paper introduces a multi-objective periodic routing problem in the context of cash transportation, which attempts to increase security by generating unpredictable alternative paths and spreading arrival times at each demand node. The current study covers the shortcomings of previous models on dissimilar routing and cash transportation problems from several aspects. The studied problem has tri objectives, including completion times, risk of robbery, and customers' satisfaction level considering the effects of traffic congestion as a daily phenomenon. On top of these, we extend the studied routing problem in multigraph setting, which can keep a set of efficient paths with multiple attributes (e.g., risk, time). Such representation enables us to evoke dissimilar route plans not only by reordering the sequence of nodes but also by employing alternative links even in a fix sequence of nodes. To handle the computational challenges arising from these properties, we propose a new evolutionary algorithm based on NSGA-II. The proposed method is embedded with a fuzzy logic technique to guide the applied operators and benefits from caching memory to accelerate and diversify the searching process. The results of implementing the proposed algorithm on test instances confirm the effectiveness of our method in comparison to standard NSGA-II. In addition, our performed sensitivity analyses show that the multigraph setting can substantially improve the quality of solutions with respect to all studied objectives.

Keywords: *Periodic transportation; Dissimilar vehicle routing problem; Cash-In-Transit; Path flexibility; Risk management*

1. Introduction

Nowadays, although electronic payment mechanisms (e.g., payment cards, online transactions, and mobile applications) continue to grow, currency is still the most frequently used payment instrument. Indeed, over 2.5 billion of adult population around the world are unbanked and do not have any access to financial services (Xu et al. 2019); thus, people especially in developing countries, prefer to use the cash as a payment method in their daily transactions. A recent report conducted by Federal Reserve in July 2020, named Diary of Consumer Payment Choice (DCPC), implies that 26% of total payment transactions in the year 2019 and 47% of small-value purchases (under \$10) were in cash. Moreover, cash was used for 47% of payments between \$10 and \$25 (Federal Reserve 2020).

In the developed countries, despite lawmakers' support to use non-cash instruments, the amount of cash in circulation (CIC) continues to grow steadily (annually from 4% to 7%) over the last five years. As an example, the CIC rate in the US is increased over 42.2% between 2005 and 2014. China tackles with higher rates of CIC and has experienced over 124% increase in CIC in the past decade (Xu et al. 2019). As might be expected, cash swirling is drastically high in countries that undergo distress such as Mozambique, Ukraine, and Myanmar (Cappgemini 2019).

2 This situation has led the related organizations to manage the currency supply chains in an efficient way as a
3 significant concern. In this regard, currency issuance, its transportation, inventory management, disposal operations,
4 and other involved handling fees affect the total costs of currency supply chains especially when a country is faced
5 by a high inflation rate (Geismar et al. 2017). Hence, a secure transportation is an essential and unavoidable
6 component of cash supply chain, which can be very costly and risky. The worldwide annual cost of handling cash,
7 which is estimated to be over 300 billion dollars, implies the importance of this matter (Talarico 2016).

8 In this work, we focus on the modeling and treatment of a real-life application concerning the periodic secure
9 distribution of cash and valuable items in urban areas. In general, Cash-In-Transit (CIT) companies should consider
10 several conflicting objectives (e.g., risk, cost, time, etc.) in their routing plans. Among different versions of Vehicle
11 Routing Problems (VRPs) that have been proposed to model the real-life applications, CIT routing problem has only
12 received a little attention so far. However, proposed models in this filed are also not practical because they are not
13 pertinent to real-life problems. For example, since the transportation links in CIT routing problem have multiple
14 inherent attributes including travel time (cost) and traveling risk, ignoring the non-dominated alternative links in
15 the transportation model yields to lose potential feasible solutions. To capture the path flexibility, the multigraph
16 network is applied in the literature (see, e.g., Garaix et al. 2010), which is an applicable way to keep track of trade-
17 offs between the defined attributes. Herein, we study the path flexibility through the multigraph setting to benefit all
18 possible options in the routing plans. Moreover, we address a periodic version of the problem because the tasks of
19 one CIT company is scheduled over several days and the demand nodes are typically visited more than one time
20 during the planning horizon (e.g., one week) (Michallet et al. 2014). It is noteworthy that vehicle routes in different
21 periods should be planned carefully because successive use of similar routing patterns can be unsafe in practice.

22 In what follows, we explicitly discuss the attributes of transportation links associated with real-world cash
23 transportation process in urban congested areas. First, related works in the CIT routing operation assume constant
24 travel time for each link throughout a day, which contradicts with the real-life situations. In this study, we assume
25 that the travel time of passing each link is a time-varying parameter, which depends on both the workday of the
26 planning horizon and vehicle departure time from an origin node. Clearly, using high-congested links increase the
27 total completion time and can affect the level of security. Second, the risk formula in the literature is mostly
28 interpreted as a cumulative risk index, which varies proportionate to the length of employed links and the amount
29 of cash/valuables in vehicles (Talarico et al. 2015a, Talarico et al. 2017a, b).

30 In addition to the aforementioned factors, this study incorporates three other important vulnerable points in the
31 risk assessment of the distribution process, including (i) designing dissimilar routing plans for different periods
32 considering non-dominated multi-attribute alternative links; (ii) diversifying the moment of arrival at demand nodes
33 in different periods; (iii) considering the characteristics of the parallel links, which can significantly affect the risk of
34 the robbery occurrence. The problem at hand is modeled as a periodic time-dependent secure transportation
35 problem with path flexibility, which is abbreviated with PTDSTP-PF. This study explicitly provides several
36 contributions to the literature as shown below.

- 37 • This is the first study that investigates the time-dependent CIT routing and scheduling problem under a
38 multi-period planning horizon. The proposed model adheres First-In-First-Out (FIFO) consistency and
39 provides dissimilar and safe routing plans for delivering valuable goods in urban areas.
- 40 • While a fully connected graph is an oversimplified abstraction for presenting the road structure in urban
41 environments, a multigraph is used to represent the transportation network in the PTDSTP-PF. By this, the
42 trade-offs between different attributes of links are considered.
- 43 • The proposed PTDSTP-PF aims at minimizing three objectives pertaining (i) minimizing the total completion
44 times, (ii) minimizing the risk of carrier operations, and finally (iii) maximizing the customers' satisfaction
45 level.

- Since it is computationally difficult to solve the PTDSTP-PF, we develop a multi-objective evolutionary algorithm called fuzzy logic guided non-dominated sorting caching genetic algorithm (FL-NSCGA-II) coupled with innovative techniques to solve the problem.

The remainder of the paper is outlined as follows. In Section 2, we review the cash transportation problem and closely related works. Moreover, the literature that captures multigraph setting in routing applications is discussed. In Section 3, first, the problem is formally described, and required preliminaries are presented. Then, the PTDSTP-PF is formulated as a mixed-integer non-linear program (MINLP) in Section 4. Section 5 provides the proposed solution methodology whereas computational experiments are presented in Section 6. Section 6 also presents managerial insights derived for practitioners. Finally, conclusions are stated in Section 7.

2. Literature review

The most related vehicle routing problem to our work is the periodic vehicle routing problem (PRVP). In the PVRP, distribution (or collection) routes are constructed over a horizon of several periods and customers are generally served multiple times. This problem was introduced by Beltrami and Bodin (1974) and has several real-world applications such as waste collection, replenishment of vending machines, food distribution, etc. A vast literature studied the PVRP and its variants, see e.g., Cacchiani et al. (2014), Luo et al. (2015), Dayarian et al. (2015), Archetti et al. (2017) and Chen et al. (2019). However, only a few papers including Michallet et al. (2014), Bozkaya et al. (2017), and Hoogeboom and Dullaert (2019) addressed security issues in PVRP. Michallet et al. (2014) and Hoogeboom and Dullaert (2019) studied the arrival time variability at each customer node to increase the security in high-value transportation activities. Bozkaya et al. (2017) worked on periodic cash shipment in a bi-objective transportation model. Interested readers are referred to Francis et al. (2008) and Campbell et al. (2014) for surveys on modeling and solution approaches of PRVP.

2.1. VRPs in multigraph setting

Multigraph representation has drawn the researchers' attention in recent years in two directions.

First, several works utilized multigraph network to consider the trade-offs between the attributes of links according to Garaix et al. (2010). Multigraph network with multi-attribute links increases the computational challenges because additional operational decisions should be made to determine the path. Originally, Garaix et al. (2010) evaluated the impact of multigraph modeling in the solution of VRP. The authors assumed multiple attributes including time and cost for each link of a network and indicated that simple graph representation cannot handle the alternative paths with different compromise between the attributes. Reinhardt et al. (2016) formulated a VRP with time windows (VRPTW), considering a fixed cost for accessing each set of links. The authors discussed the problem in both multigraph and simple graph cases. In another study, Lai et al. (2016) addressed a VRP in a multigraph structure under a time restriction. They combined a Tabu search algorithm with a heuristic arc selection method to tackle the problem. Later, Koç et al. (2016) modeled a VRP where the arcs have different distances and speed limits. The aim of the model is to minimize the total depot, number of vehicles, and routing cost. The authors did not consider time-dependency in their transportation model. In another study, Behnke and Kirschstein (2017) modeled an emission-minimizing VRP with heterogeneous vehicles paying attention to the effects of path selection in which roads are differed by their speed limits and acceleration frequency. Ticha et al. (2017) studied the impact of multigraph setting in VRPTW. They developed a branch-and-price algorithm to solve their problem. Since the structure of multigraph substantially increases the computational times, Ticha et al. (2019) hybridized adaptive large neighborhood search with dynamic programming to efficiently handle the problem. Basso et al. (2019) worked on electric VRP which involves path details like speed profile and topography to estimate energy demand. Recently, Bruglieri et al. (2019) extended the green VRP with path selection decisions. They imposed a maximum duration constraint on vehicle routes and assumed that fuel consumption is proportionate to travel distance with an input

constant rate. Hiermann et al. (2019) integrated vehicle selection in electric and plug-in hybrid VRPs. Recently, Behnke et al. (2020) formulated an emission-oriented VRP on a multigraph and proposed a column generation algorithm to solve it.

To tackle multi graph representation in VRPs, other works employed the multigraph structure in a time-dependent network based on Setak et al. (2015). In this problem, due to time-varying traffic congestion, passing a longer alternative link between two specific nodes might require shorter times. Accordingly, the best link among a set of alternative options can be estimated based on the departure time at an origin node. Later, Alinaghian and Naderipour (2016) and Setak et al. (2017) modeled the time-dependent VRP (TDVRP) in a multigraph with the aim of minimizing fuel consumption and environmental emissions in urban areas. Huang et al. (2017) evaluated the role of path flexibility in cost and fuel consumption of a TDVRP.

In a recent study, Androutsopoulos et al. (2017) considered flexibility in path optimization in a bi-objective vehicle routing considering trade-offs between travel time and fuel consumption. Similar to Huang et al. (2017), Ehmke et al. (2018) explored the efficiency of alternative paths in a time-dependent routing model with a novel fuel minimization objective. Raeesi and Zografos (2019) studied multi-trips decision making in pollution-routing problem considering both business and environmental objectives on road networks. Gmira et al. (2020) developed an improved Tabu search algorithm to solve the problem of Setak et al. (2015).

Only two recent papers in the literature considered time-dependency as one of the defined attributes of arcs in a multigraph structure. Tikani and Setak (2019) focused on time-critical distribution problem in inter-city areas after disaster conditions. They assume that each link has two associated features including time-dependent traffic congestion and reliability. Furthermore, Hu et al. (2019) considered multiple paths with different traffic restrictions, transportation risk and cost in transporting hazardous materials. Figure 1 summarizes the VRPs in multigraph setting according to the introduced categorization and shows the structure of our routing model in comparison to the literature. It is necessary to mention that current work is the first study that concentrates on the applicability of multigraph network in multi-period route planning applications.

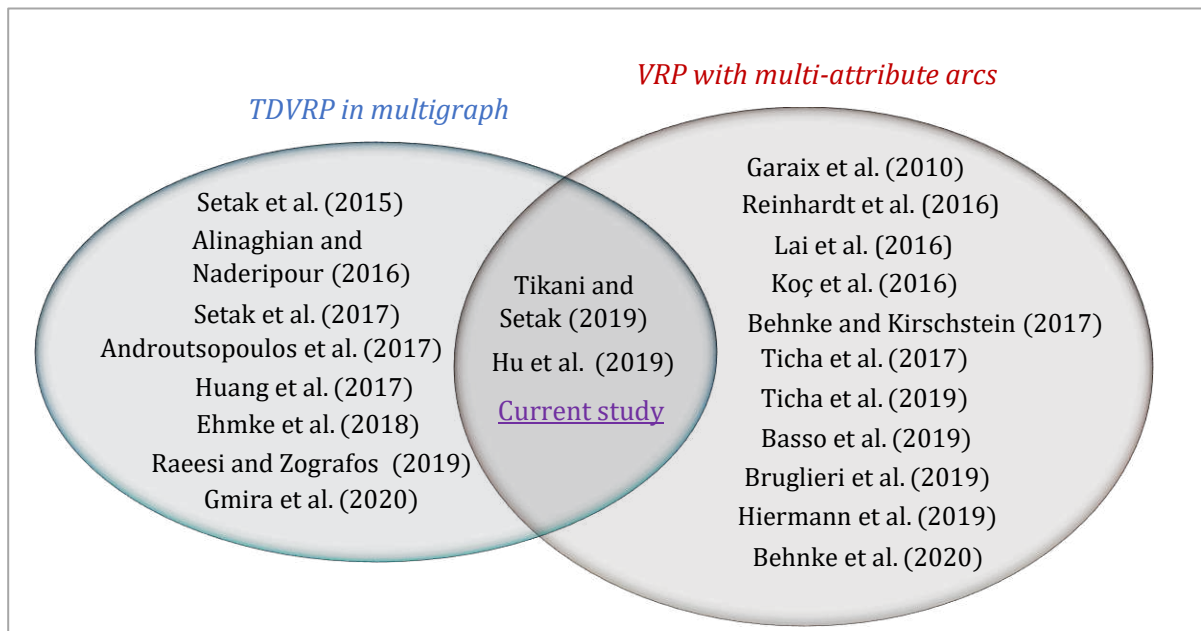


Figure 1. The overview of VRP studies with multigraph structures

2.2. Cash transportation problem

2 The CIT routing carrier is introduced as one of the relatively novel research filed in VRPs. This problem brings
4 security concern in planning of the vehicle routes. Only a few studies in the literature have focused on this important
6 issue. Calvo and Cordone (2003) proposed a single-objective model based on multiple traveling salesman problem
to manage an overnight security service. Ngueveu et al. (2010) developed an m -peripatetic VRP, which aims at
determining a set of unpredictable routes over multiple periods.

8 Yan et al. (2012) formulated a multiple-commodity network flow model for cash transportation problem in
which the concept of similarity in time and space is taken into consideration by a constraint. Later, Talarico et al.
(2013) proposed a risk-constrained CIT routing problem considering hard time windows. Michallet et al. (2014)
10 focused on a periodic VRP with time spread constraint on arrival times. Each demand point in this model is served
repeatedly during the planning horizon, and the time of reaching a node must be more than a predefined value over
12 successive periods. Talarico et al. (2015a) proposed several metaheuristics to solve a risk-constrained cash
transportation problem.

14 Later, Talarico et al. (2017a) provided a bi-objective model and a solution approach to generate safe and low-
cost vehicle routes for CIT companies. Talarico et al. (2017b) devised an improved metaheuristic by combining ant
16 colony heuristic and large neighborhood search to efficiently tackle the model of Talarico et al. (2015a). Bozkaya et
al. (2017) considered the periodic cash transportation problem with pickup and deliveries. They utilized a risk index
18 composing predictability of route and the risk of a solution. Radojičić et al. (2018a) presented a fuzzy hybrid
algorithm based on a greedy randomized adaptive search procedure improved by path relinking to cope with the
20 model of Talarico et al. (2015a). In another work, Radojičić et al. (2018b) incorporated the fuzzy theory in risk
calculation of Talarico et al. (2015a) as a new mathematical model. Hoogeboom and Dullaert (2019) focused on a
22 new solution method to diversify the arrival times in a periodic security routing problem. Recently, Xu et al. (2019)
developed a mixed-integer linear model for optimizing the distribution of different cash denominations. Repolho et
24 al. (2019) studied a variant of VRP which aims to minimize transportation and cargo theft costs in high theft risk
areas. Ghannadpour and Zandiyeh (2020) developed a bi-objective VRP with time windows in order to
26 simultaneously minimize the risk of transfers and the total distance traveled by vehicles. Soriano et al. (2020)
investigated the problem of Hoogeboom and Dullaert (2019) thorough a multigraph network. Their results show that
28 multigraph extension yields significant distance savings in comparison to the simple graph structure. Fallah-Tafti et
al. (2020) proposed a bi-objective location-routing and inventory problem in the CIT sector.

30 Other studies in the literature like Martí et al. (2009), Talarico et al. (2015b), Talarico et al. (2015b), Zajac
(2016), Constantino et al. (2017) and Zajac (2018) concentrated on the dissimilar routing problem. The aim of these
32 works is proposing several potential routes for a carrier operation according to a defined dissimilarity metric. In
detail, the cumulative risk along routes is not considered in these works. In the context of cash transportation, two
34 studies including Van et al. (2016) and Larrain et al. (2017) are focused on recirculation of cash and inventory
management in a multi-period planning horizon. Van et al. (2016) addressed an inventory-routing problem with
36 pickups and deliveries for replenishment of automated teller machines (ATMs). While Larrain et al. (2017) proposed
an inventory-routing problem considering cassettes and stockouts. The authors prepared a novel hybrid algorithm
38 to solve their problem. It is worth noting that these two works did not consider any risk aspect of transportation.
Table 1 indicates the features of our CIT routing model comparing to the closely relevant studies in the literature.

40 Despite recent efforts in taking the risk aspects in CIT routing problems, existing models cannot precisely reflect
the real-world concerns. These models are able to identify only a subset of the eligible potential paths without
42 considering congestion effects in inner-city areas. Consequently, there exists an open research issue in the CIT sector
to recognize optimal safe paths in urban roadway networks. This paper strives to fill this gap by studying a new
44 routing model for transportation of cash and valuables by safe and dissimilar routing plans.

Table1. Summary of studies in transportation of cash (or valuable goods)

Reference	Objective(s)			Vehicle capacity	Multi-period planning	Time window	Risk features			Arrival time diversification	Transportation Network	Customer satisfaction	Traffic congestion	Solution algorithm
	Single	Multi	Item(s)				CRR	UFL	MAA					
Yan et al (2012)	✓	-	\mathcal{C}	-	-	-	-	✓	-	✓	SG	-	-	A heuristic method based on decomposition/collapsing technique
Talarico et al (2013)	✓	-	\mathcal{C}	-	-	✓	✓	-	-	-	SG	-	-	Two metaheuristics
Michallet et al. (2014)	✓	-	\mathcal{C}	✓	✓	✓	-	-	-	✓	SG	-	-	Multi-start iterated local search
Talarico et al (2015a)	✓	-	\mathcal{C}	-	-	-	✓	-	-	-	SG	-	-	Metaheuristics
Van et al. (2016)	✓	-	\mathcal{C}	✓	✓	-	-	-	-	-	SG	-	-	Branch-and-cut with valid inequalities
Talarico et al (2017a)	-	✓	\mathcal{C}, \mathcal{R}	✓	-	-	✓	-	-	-	SG	-	-	A hybrid meta-heuristic
Bozkaya et al. (2017)	-	✓	$\mathcal{PL}, \mathcal{R}$	✓	✓	✓	-	✓	-	✓	SG	-	-	Adaptive randomized path selection algorithm
Talarico et al (2017b)	✓	-	\mathcal{C}	✓	-	-	✓	-	-	-	SG	-	-	A Large neighborhood meta-heuristic
Larrain et al. (2017)	✓	-	\mathcal{C}	✓	✓	-	-	-	-	-	SG	-	-	Variable MIP neighborhood descent
Radojičić et al (2018a)	✓	-	\mathcal{C}	-	-	✓	-	-	-	-	SG	-	-	Fuzzy greedy randomized adaptive search procedure
Radojičić et al (2018b)	✓	-	\mathcal{C}	-	-	✓	-	-	-	-	SG	-	-	Optimization package CPLEX
Hoogeboom and Dullaert (2019)	✓	-	\mathcal{C}	✓	✓	✓	-	-	-	✓	SG	-	-	Iterated granular Tabu search
Xu et al. (2019)	✓	-	\mathcal{C}	✓	-	-	✓	-	-	-	SG	-	-	Hybrid Tabu search
Repolho et al. (2019)	✓	-	\mathcal{C}	✓	✓	✓	-	-	-	-	SG	-	-	Simulated annealing metaheuristic
Fallah-tafti et al. (2019)	-	✓	\mathcal{C}, \mathcal{R}	✓	✓	✓	-	-	-	-	SG	-	-	ϵ -constraint method
Soriano et al. (2020)	✓	-	\mathcal{C}	✓	✓	✓	-	-	-	✓	MG	-	-	An adaptive large neighborhood search
Ghannadpour and Zandiyeh (2020)	-	✓	$\mathcal{C}, \mathcal{PL}$	✓	-	✓	-	-	-	-	SG	-	-	Game theoretical Multi-Objective Genetic with Large Neighborhood Search
This paper	-	✓	$\mathcal{CT}, \mathcal{R}, \mathcal{CS}$	✓	✓	✓	✓	✓	✓	✓	MG	✓	✓	Multi-objective evolutionary algorithm FL-NSCGA-II

Objective (s): \mathcal{C} (cost), \mathcal{R} (transportation risk), \mathcal{PL} (total path lengths), \mathcal{CT} (total completion times), \mathcal{CS} (customer satisfaction); Risk features: CRR (cumulative route risk), UFL (usage frequency of links), MAA (multi-attribute arcs); Transportation network: SG (simple graph), MG (multigraph).

3. Problem definition and preliminaries

The PTDSTP-PF concerns a multi-period carrier operation for delivering valuable goods from a central depot to a set of customers that are geographically dispersed in an urban area. We considered a homogeneous fleet of armored vehicles with capacity of Q provided that all vehicles must return to the depot after completing their operations. The underlying road network is modeled as a multigraph, $G = (V, E)$, where V includes depot and a set of customer nodes $N = \{1, \dots, n\}$. Moreover, $E = \{(i, j, m) : i, j \in V, i \neq j\}$ denotes the set of arcs between every node pairs. In this regard, the m^{th} alternative link between two nodes i and j is given by $(i, j, m) \in E$. The parallel links are differentiated by the following attributes; multiple traffic conditions, which vary temporally during a day; and different traveling risks, which is estimated based on link characteristics (e.g., tunnels, lane width), usage frequency of the link, socio-economic status of the region, etc.

It can be seen that employing similar routing plans on different periods of a planning horizon is undesirable due to security considerations. Therefore, the proposed PTDSTP-PF strives to identify dissimilar and safe routing schemes for each period taking special attention to available alternative links in a multigraph network. Before describing the mathematical formulation, we expressed the nomenclatures and preliminary fundamentals related to the problem in Table 2.

The proposed PTDSTP-PF formulation uses two sets of binary variables (y_{ik}^p, x_{ijm}^{hkp}) and five non-negative variables ($t_{ik}^p, R_{ik}^p, S_i^p, \Gamma_{ijm}^p, C_{ik}^p$). Binary variable y_{ik}^p with $\forall i \in N$ takes 1 if demand node i is served by vehicle $k \in K$ in period $p \in P$. Binary variable x_{ijm}^{hkp} equals to 1 if the m^{th} link between node i and j in the h^{th} time interval of period p has been traversed by vehicle k . Moreover, variable t_{ik}^p indicates the departure time of vehicle k from demand node i in period p . Variable R_{ik}^p presents the cumulative risk that vehicle k incur after visiting node i in period p . Variable S_i^p is used to determine the service satisfaction level at customer node i in period p . Furthermore, the Γ_{ijm}^p represents the robbery risk per unit of time for the link (i, j, m) in period $p \geq 2$. Finally, variable C_{ik}^p equals to the amount of remaining valuables in the vehicle k at node i in period p .

Table2. Notations and definitions

Sets and indices

N	Set of demand nodes $N = \{1, \dots, n\}$;
$\{0 \cup n + 1\}$	Depot node (and its dummy node);
i, j	Set of nodes represented by $i, j \in \{N \cup 0 \cup n + 1\}$;
N_{VIC}	A subset of demand nodes including very important customers $N_{VIC} \in N$
N_{IC}	A subset of demand nodes including important customers $N_{IC} \in N$
K	Set of vehicles represented by $k \in \{1, \dots, K \}$;
P	Set of periods in the planning horizon represented by $p \in \{1, \dots, P \}$;
M_{ij}	Set of alternative links between two vertices i and $j, i \neq j$ represented $m \in \{1, \dots, M_{ij} \}$.

Input parameters

D_i^p	The demand of node i at period p ;
s_i	The service duration time for serving demand node i ;
Q	Capacity of a homogeneous vehicle;
f_i^p	Binary parameter, 1 if demand node i should be served in period p ;
L	The latest allowable service time for all customer nodes;
φ	Latest desirable arrival time for set $\{N_{VIC} \cup N_{IC}\}$
δ_{ijm}	The robbery risk per unit of time for a link (i, j, m) in the first period;

ξ_i	The time spread threshold for arrival time at node i for periods $p > 1$;
ψ_{ijm}	The risk intensity factor for reusing a link (i, j, m) ;
\bar{T}_{ijm}^{hp}	The head points in the travel time function for the m^{th} link between two vertices i and j in period p ;
$a_{ijm}^{hp}, b_{ijm}^{hp}$	Coefficients for determining travel time in the h^{th} time interval along the m^{th} link between vertices i and j in the period p .

3.1. FIFO property in time-dependent networks

The FIFO property prevents surpassing on the links in a time-varying network. It assures for two identified vehicles if one of them leaves the origin location earlier, it will reach the destination before the subsequent one. Earlier studies on TDVRP (e.g., Ichoua et al. 2003) considered extra simplification in reflecting congestion level by using a discrete time function to acquire travel time, which does not adhere to FIFO property. An example of a discrete time function is presented in Figure 2(a). According to the figure, if a vehicle leaves the origin node at 4:30 PM, it will arrive at its destination in 150 miles away at 9:30 PM. However, if a vehicle leaves at 6:00 PM, it will reach the destination at 9:00 PM. It is obvious that this situation does not occur in reality. To address this shortcoming, travel speed functions are converted to continuous travel time functions to accurately model the real-world conditions.

Here, we applied the method of Setak et al. (2015) to acquire the continuous travel time function for each link. The input of the method for each link (i, j, m) , and each period p is a set of T^p initial time intervals with different travel speeds. The algorithm gives h new time intervals \bar{T}_{ijm}^{hp} , with two coefficients, a_{ijm}^{hp} and b_{ijm}^{hp} . Then, if the vehicle k starts to go from node i to j at time t_{ik}^p (in the h^{th} time interval) using the m^{th} alternative link in period p , the departure time at node j can be estimated by Equation $t_{jk}^p = a_{ijm}^{hp} + b_{ijm}^{hp} \times t_{ik}^p + s_j$. Figure 2(b) shows the travel time function induced by travel speeds patterns in Figure 2(a).

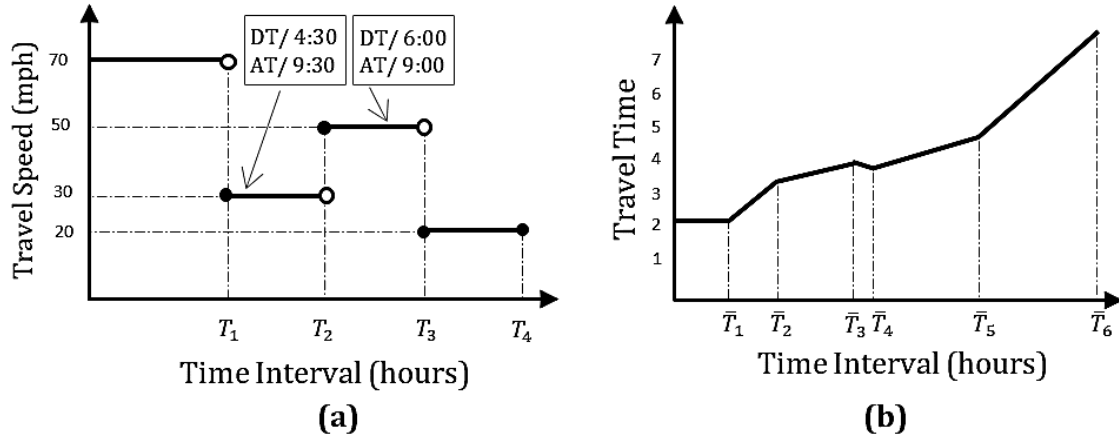


Figure 2. (a) Travel speed pattern; (b) Travel time function induced by travel speed pattern (DT: departure time; AT: arrival time).

3.2. Multi-attribute alternative links in PTDSTP-PF

The prevailing studies in VRPs involve the problem in a simple graph network. Such networks does not have efficient representation when multiple attributes are defined for the links (see Ticha et al. 2017). To overcome this deficiency, multigraphs are applied to handle the trade-offs between the attributes by keeping a set of efficient links among nodes. Thereby, a carrier is capable of switching among available links according to objectives. In this paper, the alternative links in a multigraph hold two attributes including robbery risk and time-varying traffic condition. As

it has been argued by Setak et al. (2015), depending on the departure time at each origin node, the best link with lower travel time may change. However, in the PTDSTP-PF both traffic condition and the risk of transportation, and reuse of links certainly affect the link selection. Figure 3 represents a multigraph network with multi-attribute alternative links where the links with shorter travel time can be changed based on different time intervals. The variation in travel times affects the risk of traveling along each connection.

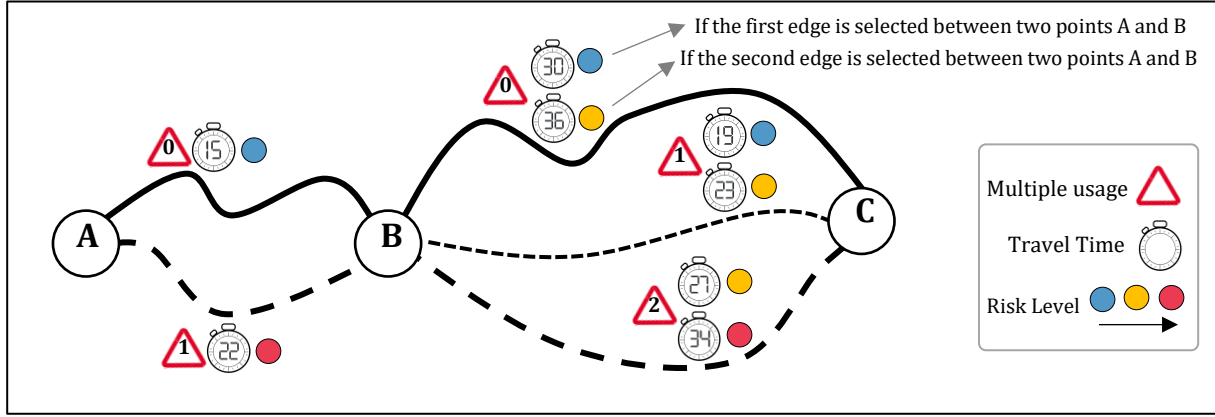


Figure 3. A transportation network with multi-attribute alternative links in periodic case

3.3. Customer satisfaction level

The lack of banknotes to cover customers' withdrawal at a bank branch or an ATM is highly relevant to customers' satisfaction. Accordingly, economic organizations tend to receive their demands as soon as possible to prevent inconvenience to the final customers. In what follows, we used *customer* for organizations or ATMs, which are directly involved with the CIT company. In the PTDSTP-PF, a hard time windows setting is incorporated as a constraint and the customer satisfaction is addressed as one of the optimization objectives. Equation (1) is applied to assure all vertexes are served before the special time L in which $\sum_{k \in K} t_{ik}^p$ represents the service completion time at customer i .

$$\sum_{k \in K} t_{ik}^p \leq L \quad \forall i \in N, \forall p \in P. \quad (1)$$

In practice, customers are not the same as each other in terms of their preferences. For this reason, we classified them into three groups including very important (N_{VIC}), important (N_{IC}), and casual customers (N_{CC}) where $\{N_{VIC} \cup N_{IC} \cup N_{CC}\} = N$. We assume that the time of completing services for casual customers is not critical. Therefore, a fuzzy membership function is prepared to reflect the satisfaction rates for customer set $\{N_{VIC} \cup N_{IC}\}$. We define the satisfaction level for customer $i \in \{N_{VIC} \cup N_{IC}\}$ in period $p \in P$ by the triangular fuzzy membership function $\mu_i^p(\sum_{k \in K} t_{ik}^p)$, which is related to the arrival time of a vehicle at each node (Ghannadpour and Zarrabi 2019). Figure 4 depicts the service level function corresponding to each customer category.

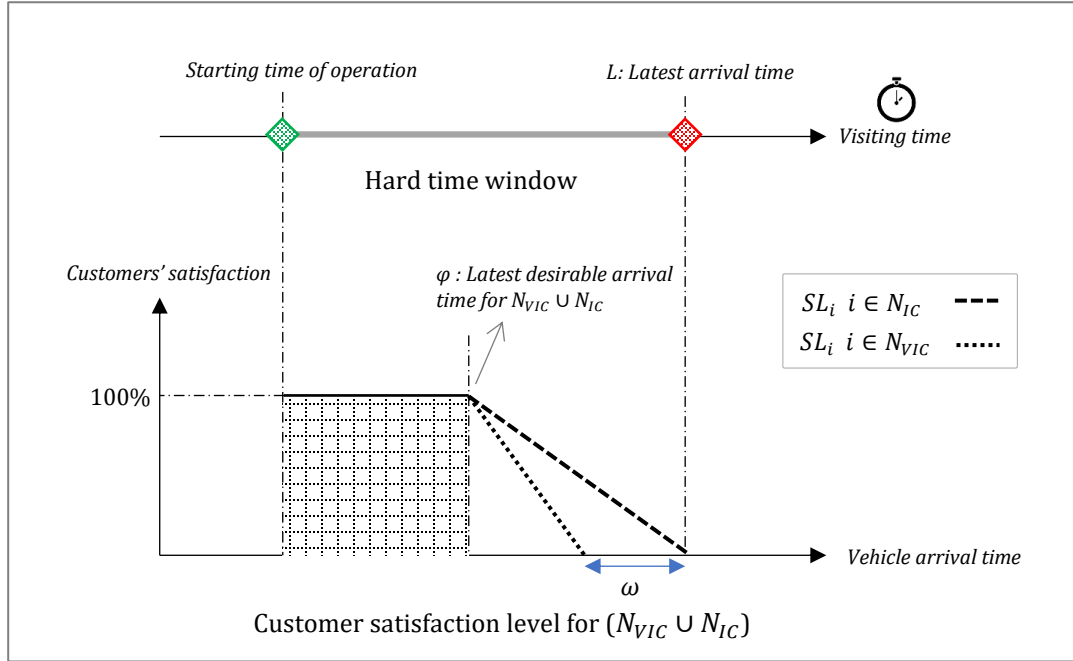
As can be seen from the figure, the grade of satisfaction for a demand node is 100%, if it is visited at its desired time; otherwise, the satisfaction grade decreases depending on the late arrival time. The satisfaction level of customer set N_{VIC} becomes zero (i.e., no satisfaction) if a carrier arrives after $(L - \omega)$. The mathematical formulation of the given approach is as follows:

$$S_i^p = \begin{cases} \mu_i^p\left(\sum_{k \in K} t_{ik}^p\right) = \left(\frac{(L - \omega) - \sum_{k \in K} t_{ik}^p}{(L - \omega) - \varphi}\right) \times 100 w_i^p + 100(1 - w_i^p) & \forall i \in N_{VIC}, p \in P, \\ \mu_i^p\left(\sum_{k \in K} t_{ik}^p\right) = \left(\frac{L - \sum_{k \in K} t_{ik}^p}{L - \varphi}\right) \times 100 w_i^p + 100(1 - w_i^p) & \forall i \in N_{IC}, p \in P. \end{cases} \quad (2)$$

2 In Equations (2-3) the variable w_i^p is employed to determine whether the arrival time at customer i in period p
 4 is before or after the latest desirable arrival time φ . This variable takes value by using constraints (4-5).

$$\left(\varphi - \sum_{k \in K} t_{ik}^p\right) \times (1 - w_i^p) + \left(\sum_{k \in K} t_{ik}^p - \varphi\right) \times w_i^p < 0 \quad \forall i \in \{N_{VIC} \cup N_{IC}\}, p \in P, \quad (4)$$

$$w_i^p \in \{0,1\}. \quad (5)$$



6 Figure 4. The fuzzy satisfaction function for each class of customers

8

3.4. Risk assessment framework

10 The transportation risk has attracted only a little attention in the CIT. On the contrary, several models in hazmat
 12 transportation captured different risk functions for traversing the links of a network. Generally, the risk function in
 14 these studies is characterized based on the nature of transported dangerous material and road conditions. Despite
 the hazmat routing problem, in CIT sector, the population is not endangered due to an explosion probability. Instead,
 each vehicle is under the risk of being robbed during the operation. We expressed the risk of robbery occurrence in
 the link (i, j, m) of a multigraph by the following involved concepts:

16

18 *Robbery rate per unit of time:* Each link of the network has different robbery probability Γ_{ijm}^p per time unit. Γ_{ijm}^p
 relies on several factors such as the condition of a link, social structure of a region, usage frequency, weather
 conditions and etc.

20 *Usage frequency:* Using repetitive transferring links during different periods induces similar routing plans in the
 22 planning horizon. In this regard, an intensity factor ψ_{ijm} is applied to penalize the recurrence of the link (i, j, m)
 in the routing plans. Setting large values for ψ_{ijm} prevents using the corresponding link in the planned routes. However,

setting $\psi_{ijm} = 0$ allows reusing the link, which in turn leads to increase the similarities. In the first period, the robbery probability of each link Γ_{ijm}^p is initially set to δ_{ij}^m (based on Equation (6)), and then in the subsequent periods, the robbery probability are computed using recursive Equation (7).

$$\Gamma_{ijm}^p = \delta_{ijm} \quad \forall i \in (0 \cup N), j \in (N \cup n + 1), m \in M_{ij}, p = 1, \quad (6)$$

$$\Gamma_{ijm}^p = \Gamma_{ijm}^{p-1} \times \left(1 + \psi_{ijm} \sum_{k \in K} \sum_{h \in H_{m_{ij}}} x_{ijm}^{hkp-1} \right) \quad \forall i \in (0 \cup N), \forall j \in (N \cup n + 1), \forall m \in M_{ij}, \forall p \in P, p \geq 2. \quad (7)$$

To clarify the performance of risk intensity factor, an illustrative example is provided in Figure 5 (a-c) which shows that reusing similar link between nodes C and F leads to increase the robbery rate in the second period proportional to the defined risk intensity factor.

Arrival time diversification: In order to schedule and design variant safe routes in the PTDSTP-PF, variations in the customers' visiting times should be considered together with the usage frequency of links. Accordingly, the arrival time at each customer node must be spread during the planning horizon (Hoogeboom and Dullaert 2019). We control the variability in arrival times using the non-linear Constraints (8). In this constraint, the parameter ξ_i is a minimum time-space variability for a demand node i that is initialized based on experts' poll.

$$\left| \sum_{k \in K} t_{ik}^p - \sum_{k \in K} t_{ik}^{p'} \right| \geq \xi_i \quad \forall i \in N, \forall p, p' \in P, p \neq p'. \quad (8)$$

In this case, assume that in the example of Figure 5 (a) the parameter ξ_A is set to 10. Figure 5 (d-e) show the time-space representation of routing plans of Figure 5 (b-c), respectively. According to the time-space diagrams, the visiting time of customer A is spread during the planning horizon to satisfy the constraint (8).

Time-dependent travel time: The probability of a robbery attack depends on time duration along the link (i, j, m) . Since the problem is studied in a time-dependent network, the travel time between two locations might vary at different time of a day. Based on the introduced notations, traveling time along the link (i, j, m) in the route k can be achieved by $(t_j^k - t_i^k - s_j)$.

Rate of success robbery: A probability v_{ijm}^p is considered to represent the success robbery rate if it occurs. Several factors may affect the success rate such as quality of employed equipment, police promptness, crew skills, etc. (Talarico et al. 2015a).

Asset loss exposure: The amount of losses that have been caused due to a successful robbery. It equals to non-delivered goods in the middle of carrier operation. Equation (9) is defined to specify the total goods that should be carried along the route k and the variable C_{ik}^p in Equation (10) gives the remain goods after visiting node j in the route k .

$$C_{0k}^p = \sum_{i \in N} D_i^p y_{ik}^p \quad \forall k \in K, \forall p \in P, \quad (9)$$

$$\sum_{m \in M_{ij}} \sum_{h \in H_m} x_{ijm}^{hkp} = 1 \Rightarrow C_{jk}^p = C_{ik}^p - D_j^p \quad \forall i, j \in N, \forall k \in K, i \neq j, \forall p \in P. \quad (10)$$

Thus, the risk of robbery event on a link (i, j, m) in period p can be calculated by:

$$\text{Robbery occurrence along link } (i, j, m) \leftarrow \Gamma_{ijm}^p \cdot v_{ijm}^p \cdot C_{ik}^p \cdot (t_{jk}^p - t_{ik}^p - s_j). \quad (11)$$

Since estimation of the success robbery rate in real conditions is very difficult, consistent with the literature (Talarico et al. 2015a) we assumed a fixed value. Therefore, in what follows the parameter v_{ijm}^p is ignored. Eventually, the variable R_{jk}^p is utilized to return the total risk of route k after passing node i through node j by link m in period p . The defined equation is as follows:

$$R_{jk}^p = \Gamma_{ijm}^p C_{ik}^p (t_{jk}^p - t_{ik}^p - s_j) + R_{ik}^p. \quad (12)$$

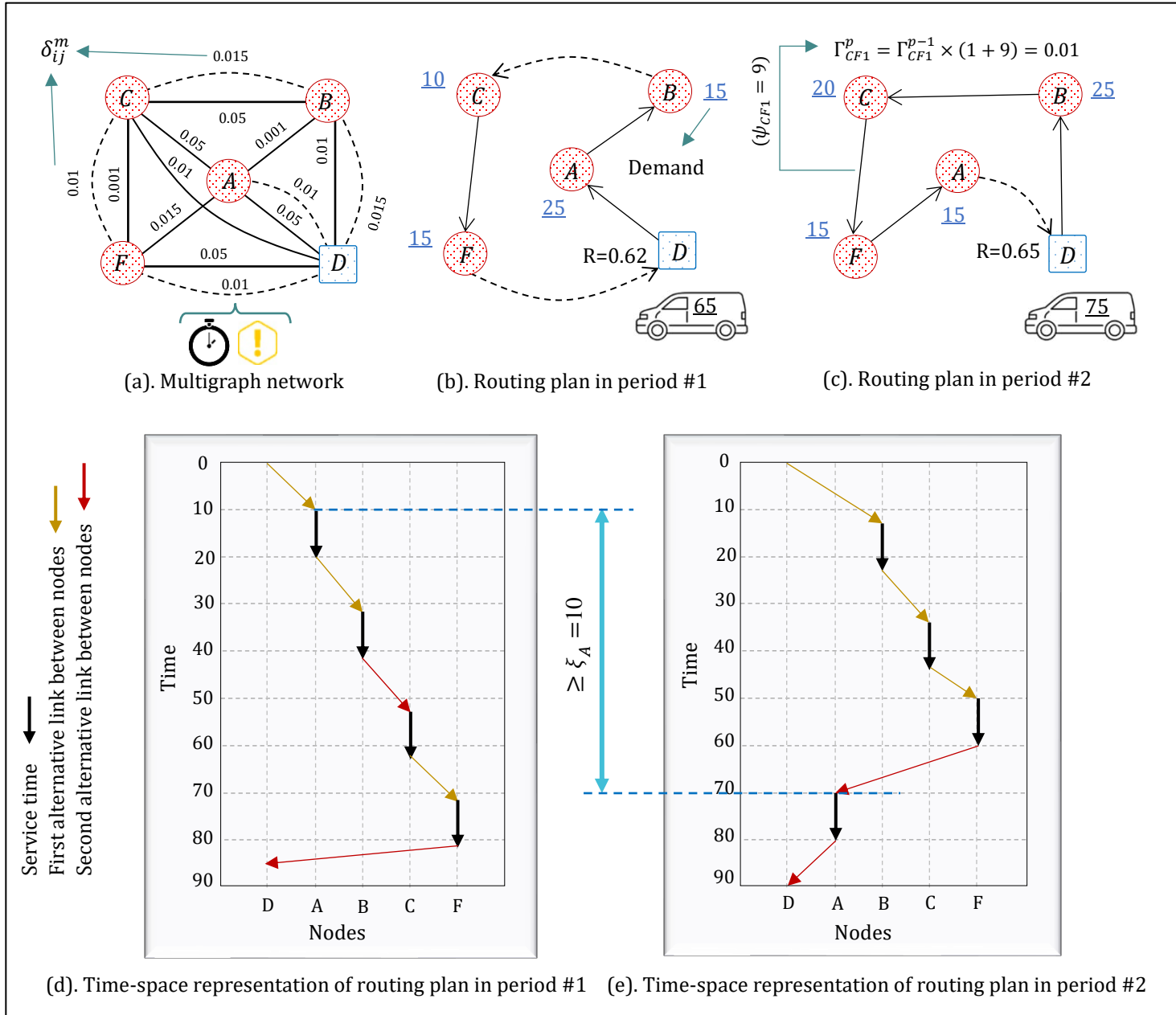


Figure 5. An illustrative example of a solution to the problem (dashed lines: parallel links)

2 Let's consider a transportation between two nodes i and j using m^{th} alternative link is shown by $i \xrightarrow{m} j$. The cumulative
 4 risk of routing plans in Figure 5 (b) and Figure 5 (c) can be computed by Equation (12) as follows:

$$\begin{aligned}
 R_{D1}^1 &= \left(0.05 \times 65 \times \frac{10}{60} \right) + \left(0.001 \times 40 \times \frac{12}{60} \right) + \left(0.015 \times 25 \times \frac{11}{60} \right) + \left(0.001 \times 15 \times \frac{9}{60} \right) + \left(0.01 \times 0 \times \frac{4}{60} \right) \approx 0.62 \\
 &\quad D \xrightarrow{1} A \quad A \xrightarrow{1} B \quad B \xrightarrow{2} C \quad C \xrightarrow{1} F \quad F \xrightarrow{2} D \\
 R_{D1}^2 &= \left(0.01 \times 75 \times \frac{13}{60} \right) + \left(0.05 \times 50 \times \frac{10}{60} \right) + \left(0.01 \times 30 \times \frac{7}{60} \right) + \left(0.015 \times 15 \times \frac{10}{60} \right) + \left(0.01 \times 0 \times \frac{10}{60} \right) \approx 0.65 \\
 &\quad D \xrightarrow{1} B \quad B \xrightarrow{1} C \quad C \xrightarrow{1} F(\text{reuse}) \quad F \xrightarrow{1} A \quad A \xrightarrow{2} D
 \end{aligned}$$

8

4. Mathematical formulation of the PTDSTP-PF

10 This section represents a MINLP model of the PTDSTP-PF. The following assumptions are respected in our
 12 proposed model: (i) a homogeneous fleet with limited capacity is taken into account; (ii) all vehicles start their
 14 operations from a single depot and at the starting points of time intervals; (iii) each vehicle performs only one route
 16 per period and returns to the depot after the assigned operation; (iv) the quantity of demands at each location's node
 and at each period is known; (v) all customers are categorized into three classes: N_{VIC} , N_{IC} , and N_{CC} in advance; (vi)
 the PTDSTP-PF is studied in urban regions. Therefore, alternative links are available to get from one node to another
 (multigraph setting).

18 The PTDSTP-PF is formulated as a multi-objective optimization problem. In the following, the objectives functions
 and the constraints related to capacity and connectivity of routing operation are described in detail.

20 Minimizing the total completion time: The first objective (13) strives to minimize the total completion times for
 all vehicles in all periods, given by:

$$f_{time} = \min \left\{ \sum_{p \in P} \sum_{k \in K} t_{n+1k}^p \right\}. \quad (13)$$

24 Minimizing the risk level: The second objective (14) strives to minimize the worst cumulative route risk faced by
 any vehicle for each period of the distribution operation. This objective is calculated by:

$$f_{risk} = \min_{p \in P} \left\{ \max_{k \in K} R_{n+1k}^p \right\}. \quad (14)$$

26 Maximizing the customers' satisfaction: As described in Section 3.3, the service level of a customer is relevant to
 28 its visiting time. The third objective maximizes the average satisfaction level of customers in set N_{VIC} and N_{IC} . This
 function can be formulated as follows:

$$f_s = \max \left\{ \frac{1}{|N_{VIC}| + |N_{IC}|} \sum_{p \in P} \sum_{i \in \{N_{VIC} \cup N_{IC}\}} S_i^p \right\}. \quad (15)$$

30 In the following, we present all constraints. The parameter E is a sufficiently large number.

$$\sum_{k \in K} y_{ik}^p = f_i^p \quad \forall i \in N, \forall p \in P \quad (16)$$

$$\sum_{i \in (0 \cup N), i \neq j} \sum_{m \in M_{ij}} \sum_{h \in H_{m_{ij}}} x_{ijm}^{hkp} = y_{ik}^p \quad \forall j \in N, \forall k \in K, \forall p \in P \quad (17)$$

$$\sum_{j \in (N \cup n+1), i \neq j} \sum_{m \in M_{ij}} \sum_{h \in H_{m_{ij}}} x_{ijm}^{hkp} = y_{jk}^p \quad \forall i \in N, \forall k \in K, \forall p \in P \quad (18)$$

$$\sum_{i \in (0 \cup N)} \sum_{m \in M_{ij}} \sum_{h \in H_{m_{ij}}} x_{ijm}^{hkp} = \sum_{i \in (N \cup n+1)} \sum_{m \in M_{ij}} \sum_{h \in H_{m_{ij}}} x_{jim}^{hkp} \quad \forall j \in N, \forall k \in K, \forall p \in P \quad (19)$$

$$\sum_{k \in K} y_{0k}^p \leq |K| \quad \forall p \in P \quad (20)$$

$$Cp_{0k}^p \leq Q \quad \forall k \in K, \forall p \in P \quad (21)$$

$$x_{iim}^{hkp} = 0 \quad \forall i \in (N \cup R), \forall m \in M_{ij}, \forall h \in H_{m_{ij}}, \forall k \in K, \forall p \in P \quad (22)$$

$$x_{i0m}^{hkp} = 0 \quad \forall i \in (N \cup R), \forall m \in M_{ij}, \forall h \in H_{m_{ij}}, \forall k \in K, \forall p \in P \quad (23)$$

$$x_{(n+1)jm}^{hkp} = 0 \quad \forall j \in N, \forall m \in M_{ij}, \forall h \in H_{m_{ij}}, \forall k \in K, \forall p \in P \quad (24)$$

$$t_{jk}^p - t_{ik}^p \geq a_{ijm}^{hp} + b_{ijm}^{hp} t_{ik}^p + s_j + (x_{ijm}^{hkp} - 1)E \quad \forall i \in (0 \cup N), \forall j \in (N \cup n+1), \forall k \in K, \forall m \in M_{ij}, \forall h \in H_{m_{ij}}, \forall p \in P, i \neq j \quad (25)$$

$$t_{ik}^p \geq Tnew_{ijm}^{hp} + (1 - x_{ijm}^{hkp})E \quad \forall i \in (0 \cup N), \forall j \in (N \cup n+1), \forall k \in K, \forall m \in M_{ij}, \forall h \in H_{m_{ij}}, \forall p \in P, i \neq j \quad (26)$$

$$t_{ik}^p \leq E \times y_{ik}^p \quad \forall i \in N, \forall k \in K. \quad (27)$$

2 We note that constraints (1-5), (6-10) and (12) need to be included. The constraints (16) assure that each demand
 4 node is visited exactly once by a vehicle, in each period. Constraints (17-19) exert the continuity of the generated
 6 routes, in each period. Constraints (20) guarantee that at most $|K|$ departures from the depot is possible at each
 8 period. The amount of goods carried by a vehicle is respected via constraints (21). Constraints (22-24) propagate the
 10 type of variables. Constraints (25) determine the departure times based on the sequence of nodes and employed
 links in a route. It also prevents sub-tours (E is a sufficiently large number). Constraints (26) and (27) ascertain the
 time intervals according to the vehicle's departure time. Constraints (1-5), (6-10) and (12) are described previously
 in section 3.

5. Solution methodology

12 The formulation of the PTDSTP-PF results in a MINLP mathematical model, which is known to be NP-Hard
 14 because it generalizes the capacitated time-dependent VRP (Kuo 2010). Moreover, the arc selection sub-problem of
 PTDSTP-PF for a specific sequence of nodes is also proved to be NP-hard (Garaix et al. 2010). Accordingly, in order
 to deal with multiple objective functions of PTDSTP-PF an optimization method based on NSGA-II is proposed to find
 a group of alternative efficient solutions called *Pareto front*. A Pareto front is composed of (non-dominated) Pareto
 optimum solutions that can be achieved by addressing the following principles (Wang et al. 2014). First, pareto
 dominance: between two solutions X_1 and X_2 , if solution X_1 is better than X_2 for at least one objective function,
 solution X_2 is then dominated by X_1 (represented by $X_1 > X_2$). Second, non-dominated solution: a solution X_1 is called
 non-dominated or Pareto optimal if and only if no solution X_2 is found that satisfies $X_2 > X_1$. And third, non-
 dominated frontier (Pareto front): a set of all Pareto optimal solutions that cannot be overridden by other obtained
 solutions.

24 A well-known metaheuristic NSGA-II based on genetic algorithm by incorporating non-dominated sorting
 method and crowded-comparison operator is proposed by Deb et al. (2002). This iterative algorithm is designated
 to simultaneously deal with multiple objectives. It starts from an initial random population of individuals and mimics
 the process of genetic evolution to create stronger members. At each iteration, a population of solutions is explored,

and the new solutions can be found. The NSGA-II uses two criteria including the rating (ranking) and the crowding distance to compare the members of two consecutive populations. In the first criterion, the individuals of a population is ranked based on the concept of domination. In this regard, the individuals of a population, which are not dominance by other members, belong to the first front. To obtain the members of the next fronts, the available solutions in the prior fronts are neglected and domination process is repeated to reach the subsequent Pareto fronts. Each member of a Pareto front with a same rank cannot dominate other members considering other objective functions. Furthermore, the crowding distance measures the diversity of populations where a higher value implies a wider diversity. More precisely the crowding distance evaluates the density of solutions around a specific solution in each population using equation (28). In this equation, Z represents the number of objectives and $f_{i+1,w}$ indicates the value i th objective function. Minimum and maximum value of the w th objective function is also represented by $f_{\min,w}$ and $f_{\max,w}$, respectively.

$$I_i = \sum_{w=1}^Z \frac{f_{i+1,w} - f_{i-1,w}}{f_{\max,w} - f_{\min,w}}. \quad (28)$$

At each iteration, a new group of individuals is populated from existing generation by employing evolutionary operators including both crossover and mutation. In the crossover operator, the characteristics of two selected parents are combined to generate new children. In addition, the mutation operator applies some certain rules to rearrange the location of genes in a chromosome and create a new individual. Similarly, an immigration operator is also employed to preserve the diversity of searching process. In overall, the parents' population, generated offsprings and immigrants are gathered as a population. Then non-dominant sorting mechanism is used to categorize the members of entire population. Finally, the next population is filled according to the performed prioritization. Since it is not possible to transfer all individuals of existing population into subsequent population, the crowding distance measure helps to fill the population in a way that solutions with lower crowding distance is prioritized for filling the next population. Figure 6 illustrates the evolutionary process of the proposed NSCGA-II.

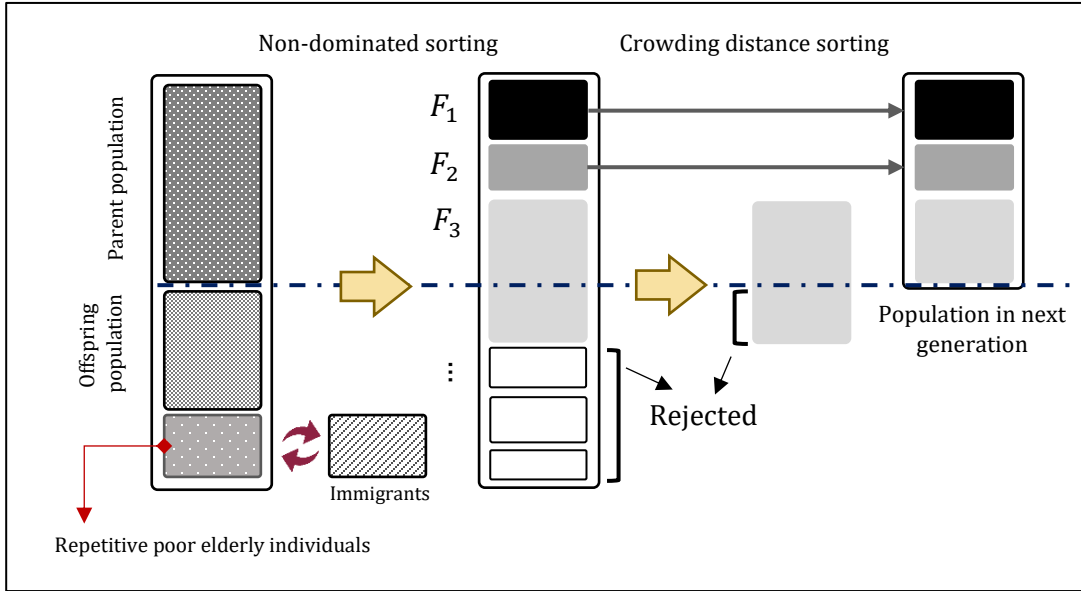


Figure 6. Evolutionary procedure of modified FL-NSCGA-II algorithm

5.1. A solution representation

The solution encoding for the PTSTP-PF is supposed to identify the assignments of customer nodes to different vehicles, the order of nodes at each constructed route and the employed edges between the nodes. For this purpose, a continuous solution representation (CSR) is used to present the individuals, which makes the exploration much smoother.

The CSR is a two-dimensional matrix $[2 \times P \times (N + K - 1)]$ including continuous numbers in the interval of $[0, 1]$. Each two consecutive rows of the matrix present the potential solution for one period. The first row determines the sequence of nodes and allocation of nodes the vehicle. While the second one represents the selected links for passing the demand nodes. In this regard, each chromosome can be decoded by two main steps:

Step 1. In this step, the continuous numbers in first row of each period should be decoded to determine the sequence of nodes and the vehicle assignments. To do this, firstly, the continuous numbers are sorted in descending order and the sequence of nodes is then determined according to the position of each number in the primary matrix.

Step 2. In the second step, the continuous numbers in the second row of each period is decoded to give the link number between every successive nodes. To do this, consider the sequence of nodes obtained from Step 1 for one period is represented by $\bar{S} = \{v_1, v_2, \dots, v_{N+K-1}\}$. Moreover, the value of a gene between two consecutive nodes v_i and v_{i+1} is presented by $g_{v_i v_{i+1}}$. Then, we select the m^{th} link between two nodes v_i and v_{i+1} if inequality $\frac{m-1}{M_{ij}} \leq$

$g_{v_i v_{i+1}} < \frac{m}{M_{ij}}$ is met. A solution representation of PTDSTP-PF and its decoding process for an example with three periods and two parallel links between nodes (i.e., $|M_{ij}| = 2, \forall i, j$) is showed in the matrices SR. Note that in the decoded matrix, the reused links are shaded. To clarify the process of **Step 2**, consider the value 0.53 in the second row of the matrix which is used to determine the link number between the depot and the first node at period 1. Here, the link $m = 1$ is not selected since the inequality $\frac{0}{2} \leq 0.53 < \frac{1}{2}$ is not met. Accordingly, the second link $m = 2$ is used as the inequality changes to $\frac{1}{2} \leq 0.53 < \frac{2}{2}$.

$$\text{SR} = \begin{array}{c} \begin{array}{|c|c|c|c|c|c|} \hline D & 0.61 & 0.44 & 0.15 & 0.86 \\ \hline 0.53 & 0.34 & 0.81 & 0.17 & 0.61 \\ \hline D & 0.92 & 0.43 & 0.19 & 0.75 \\ \hline 0.68 & 0.11 & 0.24 & 0.85 & 0.53 \\ \hline D & 0.83 & 0.59 & 0.36 & 0.27 \\ \hline 0.71 & 0.16 & 0.03 & 0.65 & 0.25 \\ \hline \end{array} \xrightarrow{\text{Decoding}} \begin{array}{|c|c|c|c|c|c|} \hline D & 4 & 1 & 2 & 3 & D \\ \hline 2 & 1 & 2 & 1 & 2 & - \\ \hline D & 1 & 4 & 2 & 3 & D \\ \hline 2 & 1 & 1 & 2 & 2 & - \\ \hline D & 1 & 2 & 3 & 4 & D \\ \hline 2 & 1 & 1 & 2 & 1 & - \\ \hline \end{array} \begin{array}{l} \text{Period \#1} \\ \text{Period \#2} \\ \text{Period \#3} \end{array}
 \end{array}$$

5.2. Evolutionary operators

Genetic operators provide the evolutionary progress of GA. In this study, for generating new potential solutions crossover, mutation and immigration operators are employed with predefined probabilities. In what follows the mechanism of these operators are described in detail.

Crossover is known as a basic genetic operator, which combine the genetic materials of two distinct parents to produce new populations. In this regard, arithmetic crossover is a useful approach since continuous numbers are used to encode chromosomes. It provides two offspring induced by linear combinations of the selected parents. Given two individuals θ_{p1} and θ_{p2} , the generated members θ_{c1} and θ_{c2} can be obtained by equations $\theta_{c1} = \lambda\theta_{p1} + (1 - \lambda)\theta_{p2}$ and $\theta_{c2} = \lambda\theta_{p2} + (1 - \lambda)\theta_{p1}$ where $\lambda \sim U(0,1)$.

Mutation operator is another reproduction mechanism in GA that prevents the searching scheme to be trapped in pure local optima. It brings new nonexistent characteristics in the population pool by some random transformations on genetic materials so as to produce better suited members. To do this, we propose four mutation schemes for changing the sequence of nodes and the suggested links between them. Then, at each mutation process, one of the defined operators is selected randomly to exchange the chromosome. The different designated operators are discussed in below:

Reverse sequence mutation: this operator randomly selects two columns within a chromosome and then inverse the contents between them. It can be applied for both sequence of nodes and the applied links among them. Matrices SR exchange to SR_{RS} if the reversion occurs between the second and fifth columns.

$$\begin{array}{c}
\begin{matrix}
SR_{RS} = \begin{bmatrix}
D & 0.61 & 0.15 & 0.44 & 0.86 \\
0.53 & 0.34 & 0.17 & 0.81 & 0.61 \\
D & 0.92 & 0.19 & 0.43 & 0.75 \\
0.68 & 0.11 & 0.85 & 0.24 & 0.53 \\
D & 0.83 & 0.36 & 0.59 & 0.27 \\
0.71 & 0.16 & 0.65 & 0.03 & 0.25
\end{bmatrix} \\
\text{Decoding} \longrightarrow \\
\begin{bmatrix}
D & 4 & 1 & 3 & 2 & D \\
2 & 1 & 1 & 2 & 2 & - \\
D & 1 & 4 & 3 & 2 & D \\
2 & 1 & 2 & 1 & \mathbf{2} & - \\
D & 1 & 3 & 2 & 4 & D \\
\mathbf{2} & \mathbf{1} & \mathbf{2} & 1 & 1 & -
\end{bmatrix} \\
\begin{matrix}
\text{Period \#1} \\
\text{Period \#2} \\
\text{Period \#3}
\end{matrix}
\end{matrix}
\end{array}$$

Two-point swap: In this operation, a new individual is generated by swapping two random columns in a chromosome. Swapping the second and fourth columns in SR yields to achieve matrices SR_S.

$$\begin{array}{c}
\begin{matrix}
SR_S = \begin{bmatrix}
D & 0.15 & 0.44 & 0.61 & 0.86 \\
0.53 & 0.17 & 0.81 & 0.34 & 0.61 \\
D & 0.19 & 0.43 & 0.92 & 0.75 \\
0.68 & 0.85 & 0.24 & 0.11 & 0.53 \\
D & 0.36 & 0.59 & 0.83 & 0.27 \\
0.71 & 0.65 & 0.03 & 0.16 & 0.25
\end{bmatrix} \\
\text{Decoding} \longrightarrow \\
\begin{bmatrix}
D & 4 & 3 & 2 & 1 & D \\
2 & 1 & 2 & 1 & 2 & - \\
D & 3 & 4 & 2 & 1 & D \\
2 & 2 & 1 & \mathbf{1} & \mathbf{2} & - \\
D & 3 & 2 & 1 & 4 & D \\
\mathbf{2} & \mathbf{2} & \mathbf{1} & 1 & 1 & -
\end{bmatrix} \\
\begin{matrix}
\text{Period \#1} \\
\text{Period \#2} \\
\text{Period \#3}
\end{matrix}
\end{matrix}
\end{array}$$

Arc exchange operator: in this operation some of the used links for a fix sequence of nodes are selected and switched by other alternative available links. For this purpose, let θ_p represents the value of a gene in a parent's chromosome, this value is replaced for the child's chromosome by equation $\theta_c = 1 - \theta_p$. The effect of arc exchange operator on the employed arcs of SR in the first and second periods is shown on matrices SR_A. Note that this operator is only usable for exchanging the available links.

$$\begin{array}{c}
\begin{matrix}
SR_A = \begin{bmatrix}
D & 0.61 & 0.44 & 0.15 & 0.86 \\
0.47 & 0.66 & 0.19 & 0.83 & 0.39 \\
D & 0.92 & 0.43 & 0.19 & 0.75 \\
0.68 & 0.11 & 0.24 & 0.85 & 0.53 \\
D & 0.83 & 0.59 & 0.36 & 0.27 \\
0.71 & 0.16 & 0.03 & 0.41 & 0.25
\end{bmatrix} \\
\text{Decoding} \longrightarrow \\
\begin{bmatrix}
D & 4 & 1 & 2 & 3 & D \\
1 & 2 & 1 & 2 & 1 & - \\
D & 1 & 4 & 2 & 3 & D \\
2 & 1 & 1 & \mathbf{2} & \mathbf{2} & - \\
D & 1 & 2 & 3 & 4 & D \\
\mathbf{2} & \mathbf{1} & 1 & 2 & 2 & -
\end{bmatrix} \\
\begin{matrix}
\text{Period \#1} \\
\text{Period \#2} \\
\text{Period \#3}
\end{matrix}
\end{matrix}
\end{array}$$

Real mutation operator: In this operator, instead of disarranging the locations of genes, some of the genes' values are replaced by new random numbers using uniform distribution $\theta_c \sim U[0,1]$. Matrices SR_R can be achieved when all genes related to the second period of SR are changed by this operator.

$$\begin{array}{c}
\begin{matrix}
SR_R = \begin{bmatrix}
D & 0.61 & 0.15 & 0.44 & 0.86 \\
0.53 & 0.34 & 0.17 & 0.81 & 0.61 \\
D & 0.08 & 0.29 & 0.61 & 0.78 \\
0.73 & 0.24 & 0.34 & 0.80 & 0.18 \\
D & 0.83 & 0.36 & 0.59 & 0.27 \\
0.71 & 0.16 & 0.65 & 0.03 & 0.25
\end{bmatrix} \\
\text{Decoding} \longrightarrow \\
\begin{bmatrix}
D & 4 & 1 & 3 & 2 & D \\
2 & 1 & 1 & 2 & 2 & - \\
D & 4 & 3 & 2 & 1 & D \\
\mathbf{2} & \mathbf{1} & \mathbf{1} & \mathbf{2} & \mathbf{1} & - \\
D & 1 & 3 & 2 & 4 & D \\
1 & \mathbf{1} & \mathbf{2} & 1 & 1 & -
\end{bmatrix} \\
\begin{matrix}
\text{Period \#1} \\
\text{Period \#2} \\
\text{Period \#3}
\end{matrix}
\end{matrix}
\end{array}$$

5.3. Penalized fitness function

One practical approach to handle the constraints in metaheuristics is allowing the existence of infeasible solutions during the search and considering their violations as penalties in the objective value. Here, arrival time diversification, the capacity constraint, and the latest allowable arrival time are allowed to be violated during the searching process. Let X be a solution for the PTDSTP-PF with objective value $OV(X)$. Then, we can compute the overload by $q(X) = \sum_{k \in K} \sum_{p \in P} \max \{ Cp_{0k}^p - Q, 0 \}$ the overtime is calculated by $t(X) = \sum_{i \in N} \sum_{p \in P} \max \{ \sum_{k \in K} t_{ik}^p - L, 0 \}$, and arrival time violation is given by $a(X) = \sum_{i \in N} \sum_{p \in P} \sum_{p' \in P, p' \neq p} \max \{ \xi_i - | \sum_{k \in K} t_{ik}^p - \sum_{k \in K} t_{ik}^{p'} |, 0 \}$. Thus, the penalized objective value is computed by $POV(X) = OV(X) + \eta_1 q(X) + \eta_2 t(X) + \eta_3 a(X)$, where parameters η_i are automatically adjusted every iteration. In detail, if one of the mentioned constraints is violated, then the related parameter η_i is multiplied by $\sigma > 1$; otherwise, it is divided by σ .

5.4. Fuzzy logic-guided approach

Several researchers like Lotfi and Kashani (2004) or Lau et al. (2009) incorporated fuzzy logic techniques into evolutionary algorithms to tackle different practical applications. In detail, these studies improved the performance of searching process by a fuzzy logic approach, which adjusts the crossover and mutation rate during the executions. Accordingly, we implement the fuzzy methods not only for adjusting the crossover, mutation rates but also for dynamically adapting the strategies of operators. In order to handle the parallel links between nodes of a multigraph, a fuzzy logic method is proposed to control the operators of FL-NSCGA-II to be mainly applied on the first row of the chromosomes' matrix (sequence of nodes) or the second row (suggested links).

Since in multigraph networks only a few numbers of parallel links are available between each pair of nodes, the cardinality of solutions in selecting proper arcs is much less than finding the best sequence of demand nodes. In the other hands, a set of good solutions is achievable only if proper arcs are selected for a group of suited nodes' sequences. To this end, it seems desirable if at the beginning of the searching process the applied operators focus on generating different sequences for demand nodes and then gradually incorporate arc exchange operations into the searching scheme. For this purpose, the fuzzy logic is employed to dynamically adjust the rates of operators after ten consecutive iterations. We applied this adjustment procedure for every ten generations since the algorithm needs a sufficient time to respond to the change (see Lau et al., 2009), which is based on the following factors:

- (i) Iteration number (it) and the total number of iterations (IT);
- (ii) Population diversity in the current iteration $d(it)$;
- (iii) The difference between average fitness values of population in the current iteration it in comparison to iteration $it - 9$. Here, in order to transform the multiple objective functions of PTDSTP-PF into a single value, we applied the sum of the objectives with normalization. Accordingly, the average fitness values of a population with normalization (f_a) can be obtained by equation (29).

$$f_a = \frac{\sum_{j=1}^{NPOP} \sum_{i=1}^3 (f_{ij} - Z_i^U) / (Z_i^N - Z_i^U)}{3 \times NPOP} \quad (29)$$

where $NPOP$ equals to the number of existing individuals, f_{ij} represents the i^{th} objective of j^{th} individual, Z_i^U shows the ideal vector of the i^{th} objective function, and Z_i^N is the related Nadir point.

- (iv) Crossover and mutation rates for both nodes' sequences and arc selection.

By this method, not only we are able to guide the searching scheme but also the premature convergence is prevented by preserving the population diversity. The structure of proposed fuzzy logic guided in FL-NSCGA-II can be modeled as Figure 7.

In order to determine the evolution of diversity among individuals of a generation, we modified the measure introduced by Lau et al. (2009). In this regard, equation (30) is proposed to calculate the average of bit difference of all pairs of individuals.

$$d(it) = \frac{1}{\left[\frac{\mathcal{N}(\mathcal{N} - 1)}{2} \right]} \sum_{i=1}^{\mathcal{N}} \sum_{j=i+1}^{\mathcal{N}} \sum_{k=1}^{\mathcal{K}} \sum_{\ell=1}^{\mathcal{M}} \frac{\delta_{ij}^{it}(\mathcal{G}_{kj}^{\ell}, \mathcal{G}_{ki}^{\ell})}{\mathcal{K} \times \mathcal{M}} \quad (30)$$

where \mathcal{N} denotes the number of individuals in each population, \mathcal{K} shows the length each row of the chromosome, \mathcal{M} represents the number of rows in chromosomes' structure. Assume that \mathcal{G}_{ki}^{ℓ} presents the value of k th gene in the ℓ th row of i th chromosome, then $\delta_{ij}^{it}(\mathcal{G}_{kj}^{\ell}, \mathcal{G}_{ki}^{\ell})$ takes 1 if $\mathcal{G}_{kj}^{\ell} \neq \mathcal{G}_{ki}^{\ell}$, 0 otherwise.

In Figure 7, P_c^{NS} and P_m^{NS} represent the crossover and mutation rates for nodes' sequences, while P_c^{NS} and P_m^{NS} represent the crossover and mutation rates for arc selection part of the chromosome. Moreover, the overall change of crossover and mutation rates in iteration $it + 1$ is shown by $\Delta P_c(it + 1)$ and $\Delta P_m(it + 1)$ which are the outputs of fuzzy logic approach. In detail, these values are used to adjust P_c^{NS} , P_m^{NS} , P_c^{NS} and P_m^{NS} according to the following equations:

$$P_c^{NS}(it + 1) = P_c^{NS}(it) + \frac{IT - it}{IT} \cdot \Delta P_c(it + 1) \quad (31)$$

$$P_c^{AS}(it + 1) = P_c^{AS}(it) + \frac{it}{IT} \cdot \Delta P_c(it + 1) \quad (32)$$

$$P_m^{NS}(it + 1) = P_m^{NS}(it) + \frac{IT - it}{IT} \cdot \Delta P_m(it + 1) \quad (33)$$

$$P_m^{AS}(it + 1) = P_m^{AS}(it) + \frac{it}{IT} \cdot \Delta P_m(it + 1) \quad (34)$$

2

Further information about the main procedures of fuzzy logic approach is described in Appendix A.

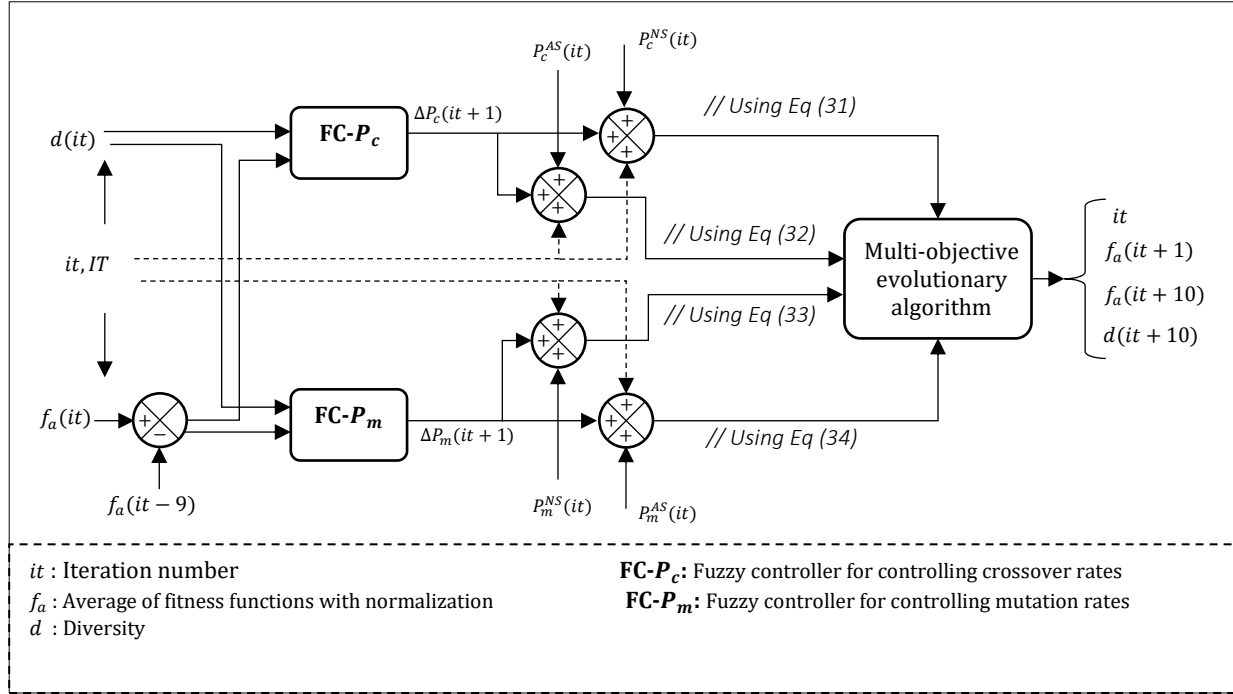


Figure 7. Structure of the fuzzy logic guided evolutionary algorithm

4

6

8 5.5. Caching technique and immigration

During the evolutionary process of the GA, it is probable that the algorithm meets same individual in different generations. Multiple evaluation of fitness values for identical chromosomes increases the overall running time. Moreover, existence of poor elderly repetitive individuals can decelerate the searching mechanism to discover unvisited promising areas in the solution space. The first step to avoid these matters is storing repetitive genetic codes in a prepared hash-queue structure with a specific limited capacity. In the following, when a new individual is generated, the algorithm, firstly checks whether the information of this individual is previously stored in the cache table. If this is the case and the individual is distinguished to be poor elderly repetitive member then this individual is replaced with a new immigrant member to explore the undiscovered regions. The main idea of this operator is inspired from its counterpart in real nature where some immigrant species get in the current population with different genetic features (Tikani and Setak 2019). Otherwise, the related objective value is evoked from hash-queue table instead of unnecessary re-calculations. An immigrant member includes none of the genetic material of current population. One individual is labeled as a poor elderly one if the following two conditions are confirmed: If existed in ten previous consecutive iterations (elderly member). And, if not belongs to the top ten percentage of stored individuals in the prepared cache table.

Let τ_{CH} shows the number of times that chromosome CH is met in τ successive generations. The details of fitness evaluation with caching method is described in Algorithm 1. Algorithm 2 is provided to expand lines 4-5 of Algorithm 1. In this algorithm, Δ_{CH} represents the number of consecutive iterations that chromosome CH has existed in

24

generations. f_i^{CH} shows the value of i^{th} objective of chromosome CH . And $SL_i^{10\%}$ reflects the fitness function (according to the i^{th} objective) of an individual which is located at the bottom of the first decile of the population in the sorted caching list.

Algorithm 1. Fitness evaluation with caching strategy

```

1  Input (chromosome  $CH$ )
2  Decode the chromosome  $CH$ 
3  If (individual  $CH$  is existed in cache memory)
4  |   If (individual  $CH$  is distinguished as a poor elderly member)
5  |   |   The individual should be replaced with a new immigrant
6  |   Else
7  |   |   Put  $\tau_{CH} \leftarrow \tau_{CH} + 1$ 
8  |   |   Update the information of cache table
9  |   End if
10 Else
11 |   Calculate the fitness value of  $CH$ 
12 |   Store the information of  $CH$  in the cache table
13 |   Sort the members (from best to worse) in the cache table according to each objective function
14 End if

```

Algorithm 2. The process of replacing a poor elderly individual with a new immigrant

```

1  Input (chromosome  $CH$ )
2  If ( $\Delta_{CH} \geq 10$ )
3  |   For  $i \leftarrow 1$  to 3 do
4  |   |   If ( $f_i^{CH} \geq SL_i^{10\%}$ )
5  |   |   |   The individual is a poor elderly one and should be replaced with a new immigrant
6  |   |   Else
7  |   |   |   break;
8  |   |   End if
9  |   End for
10 Else
11 |   break;
12 End if

```

6. Computational experiments

In this section, we first present the parameters of PTDSTP-PF to evaluate the performance of FL-NSCGA-II on randomly generated instances. All algorithms have been coded in MATLAB 2015a software on Intel Core i5 processor running at 1.8 GHz with 6 GB RAM.

6.1. Data setting

The existing benchmarks in the literature of CIT routing problem is not practical for the PTDSTP-PF due to several involved real-life concerns such as time-varying traffic congestion, multi-attribute alternative links, periodic planning, customers' satisfaction, etc. Therefore, to verify the proposed PTDSTP-PF and the developed NSCGA-II algorithm, we generate a multigraph network with 25 nodes and derive different scale instances from this network to be implemented on the model. We assume that two alternative links are available between every pair of points in the generated multigraph. The first link between two given nodes i and j is shorter but has higher traffic condition; its length equals to the Euclidean distance (E_{ij}) between two nodes i and j . While the vehicles' speed in the second parallel links is less dependent to the changes of time intervals and the lengths of links are longer than the first alternative. For this purpose, the lengths of these arcs are generated by a uniform function between two numbers [$1.1 \times E_{ij}$, $1.5 \times E_{ij}$]. The travel time functions among the nodes can be achieved by knowing the length arcs and travel speeds between them using the method of Section 3.1. The detailed information about the remainder

parameters of the model are presented in Table 3. By this, sixteen instances with different problem sizes are given in Table 4.

Table 3. Parameters used in the model

Parameter	Values	Parameter	Typical values
x_c	$\sim U[0, 20000]$	L (minutes)	$\sim U[70, 120]$
y_c	$\sim U[0, 20000]$	φ (minutes)	$\sim U[35, 60]$
D_i^p (kg)	$\sim U[10, 100]$	ω (minutes)	$\sim U[25, 35]$
s_i (minutes)	5 min	ξ_i (minutes)	5 min
Q (kg)	600 kg	Vehicle' speeds in the first link (km/h)	$\sim U[35, 55]$
δ_{ijm}	$\sim U[0, 0.2]$	Vehicle' speeds in the second link (km/h)	$\sim U[40, 70]$
ψ_{ijm}	0.1		

Table 4. Size of instances

Instance No.	1	2	3	4	5	6	7	8	9	10	11	12	13	14	15	16
Demand nodes	11	11	13	13	15	15	17	17	19	19	21	21	23	23	25	25
$ N_{VIC} , N_{IC} $	3,2	3,2	4,2	4,2	5,3	5,3	7,3	7,3	7,4	7,4	7,6	7,6	8,7	8,7	8,8	8,8
Vehicle(s)	1	2	1	2	2	3	2	3	2	3	2	3	2	3	2	3
Periods	2	3	2	3	2	3	2	3	2	3	2	3	2	3	2	3

6.2. Tuning the parameter of FL-NSCGA-II

The proposed FL-NSCGA-II algorithm has six parameters that should be tuned to increase the quality of searching process. The intended level for each parameter is presented in Table 5. Note that we determine the crossover and mutation rates for both nodes' sequence and employed arcs in the first iteration, and then these parameters are adapted according to the variety of individuals and iteration number. The results of implementing Taguchi design for the FL-NSCGA-II method is shown in Figure 8. In this figure, the candid value for each parameter is specified by a red square.

Table 5. Parameters and their level in GA. (*NPOP*: the number of population, *IT*: maximum number of iterations)

Parameter	P_c^{AS}	P_c^{NS}	P_m^{AS}	P_m^{NS}	<i>NPOP</i>	<i>IT</i>
Level #1	0.7	0.7	0.1	0.1	60	75
Level #2	0.75	0.75	0.15	0.15	80	100
Level #3	0.8	0.8	0.2	0.2	100	125

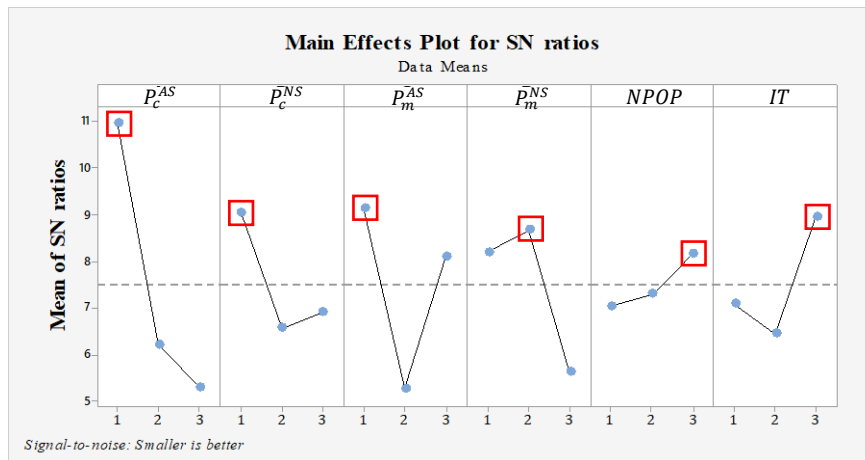


Figure 8. Signal to noise ratio chart for the parameters of FL-NSCGA-II

2 6.3. Results of the FL-NSCGA-II on instances

4 The FL-NSCGA-II provides a set of solutions as optimal (or near-optimal) Pareto frontier for each example. By
 6 this, we increase the capability of practitioners since they can choose the intended solution among the Pareto set
 8 according to their own managerial judgments. First, we present the details of results for a group of examples
 10 including 3, 7, 10 and 14, which are representative of different sizes of the instances. The Pareto frontiers of the
 12 mentioned instances are illustrated in Figure 9. The figure shows that improving one of the objectives yields to
 14 decrease the quality of two other ones. In Figure 9, the solutions A, B, and C represent the best options regarding total
 completion times, risk level and customer satisfaction, respectively. The details of the objective values are given in
 Table 6.

12 The analysis of the two solutions A and C in the studied problems shows that the manager can reach the
 14 minimum completion time but the impact on the service level would be decreased about 17% to 27%. Moreover, its
 impact on the risk level is more and equals to 51%-185%. However, we can see a meaningful trade-off between the
 risk level and customer satisfaction. In this regard, a manager can improve the risk level up to 400% by 10%-16%
 decrease in customer satisfaction rate.

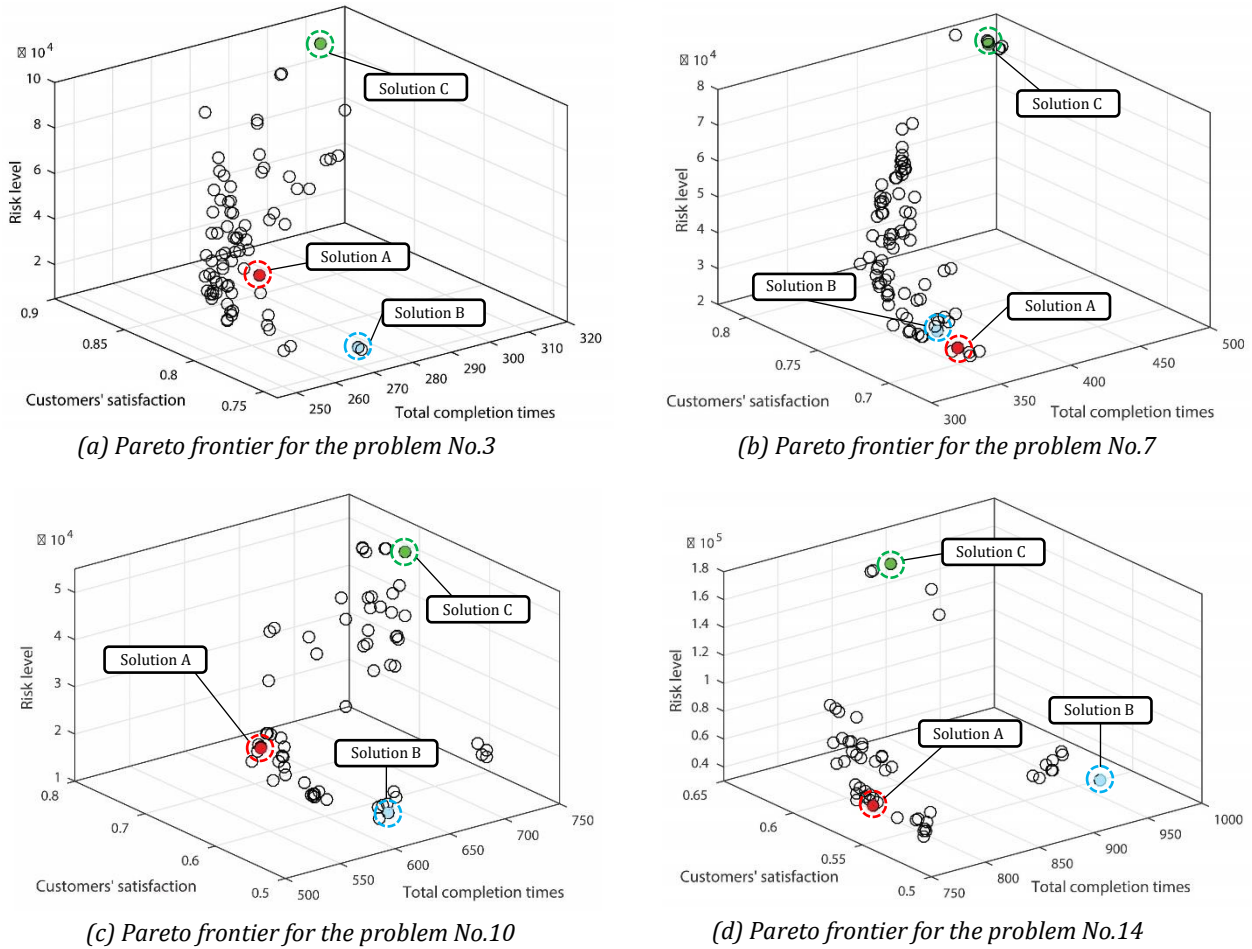


Figure 9. Pareto solutions for different problems instances.

Table 6. The best value for each objective function in Pareto front.

Instance	Objective function	The Pareto solutions			CPU time (seconds)
		A	B	C	
3	Z_1	246.84	267.76	313.21	303.61
	Z_2	53,182.07	15,651.71	86,824.21	

	Z_3	0.757	0.745	0.898	
7	Z_1	331.36	372.39	489.43	315.04
	Z_2	29,677.91	20,046.06	73,535.20	
	Z_3	0.682	0.737	0.815	
10	Z_1	514.96	617.28	741.29	322.01
	Z_2	32,831.77	13,891.45	49,691.34	
	Z_3	0.557	0.537	0.706	
14	Z_1	763.97	968.97	901.48	347.39
	Z_2	54,294.71	30,423.17	15,4851.65	
	Z_3	0.552	0.549	0.647	

2 6.3.1. Multi-objective comparison metrics

4 To measure the efficiency of FL-NSCGA-II in comparison to its pure version, we applied five well-known quality metrics from the literature. The employed metrics are explained in below (Rayat et. al 2017):

6 The number of non-dominated Pareto solutions (NOS): *larger value is better*; this metric counts the number of non-dominated solutions obtained by each algorithm. Clearly, a higher value of NOS implies that the algorithm has better exploration and can diverse the searching direction.

8 Spacing metric (SM): *smaller value is better*; this metric is used to evaluate the evenly distribution of the solution set points' along the Pareto front. The SM factor is achieved by equation $SM = \frac{\sum_{i=1}^{n-1} |\bar{d} - d_i|}{(n-1)\bar{d}}$, where n is total number of solutions in the final Pareto front, d_i represents the Euclidian distance between every successive Pareto solutions, the average of all d_i is denoted by \bar{d} .

12 Mean ideal distance (MID): *smaller value is better*; this metric computes the mean distance between the solutions of Pareto front from the ideal one. It is calculated by:

$$14 \quad MID = \frac{\sum_{i=1}^n \sqrt{\left(\frac{F1_i - F1_{best}}{F1_{Total}^{max} - F1_{Total}^{min}}\right)^2 + \left(\frac{F2_i - F2_{best}}{F2_{Total}^{max} - F2_{Total}^{min}}\right)^2 + \left(\frac{F3_i - F3_{best}}{F3_{Total}^{max} - F3_{Total}^{min}}\right)^2}}{n} \quad (35)$$

16 In equation (35), the ideal point is the best value of each objective function among all of the solutions in the Pareto front.

18 Quality metric (QM): *larger value is better*; this metric calculates the Pareto solution's percentage among all achieved non-dominated solutions from different methods, as given below:

$$20 \quad QM = \frac{\text{Number of non_dominated Pareto solutions of the method}}{\text{total number of non_dominated solutions}} \quad (36)$$

22 The denominator of QM is the non-dominated solutions acquired by the algorithms together.

24 *Computational time (CPU time)*: *smaller value is better*; this metric shows the speed of each algorithm to reach the final result.

26 The FL-NSCGA-II and its standard version (NSGA-II) are employed to solve the instances with various dimensions and the results are reported in Table 7. To have the results more visible, the obtained results are shown in Figure 10 using Boxplots. The results show that FL-NSCGA-II has a better performance compared to the NSGA-II. However, to have a more precise comparison, a statistical analysis based on the paired t-test is conducted for each metric. First the normality of all metrics SM, MID, QM, and CPU time were examined by the Anderson–Darling test, which shows that the values of all metrics are normally distributed (Nemati-Lafmejani et. al 2019). In the paired t-test, the null hypothesis indicates that the difference between obtained values of an investigated metric is insignificant, while the other hypothesis denotes that FL-NSCGA-II outperforms NSGA-II regarding the performance metric.

32 Table 8 summarizes the P-values of tests and confirmed that at 95% confidence level there exist significant differences in the given results and FL-NSCGA-II is superior to NSGA-II in the studied metrics.

34

36

Table 7. Results of the comparison metrics for different problems instances.

Instance	FL-NSCGA-II					NSGA-II				
	NOS	SM	MID	QM	CPU time (s)	NOS	SM	MID	QM	CPU time (s)
1	98	0.544	0.069	0.74	271.62	87	0.619	0.096	0.47	286.41
2	100	0.624	0.035	0.66	300.35	94	1.488	0.072	0.54	316.50
3	100	0.603	0.061	0.59	303.61	97	0.685	0.086	0.48	320.16
4	100	0.532	0.052	0.63	308.74	98	1.012	0.069	0.39	328.25
5	100	0.677	0.062	0.70	312.19	96	1.085	0.082	0.42	334.04
6	100	0.588	0.036	0.73	313.07	100	0.804	0.052	0.52	339.74
7	100	0.635	0.054	0.81	315.04	90	1.415	0.081	0.51	347.22
8	98	0.913	0.059	0.68	317.19	91	1.195	0.094	0.46	354.01
9	100	0.583	0.063	0.71	318.45	100	0.630	0.086	0.57	367.11
10	100	0.711	0.069	0.62	322.01	90	0.705	0.083	0.50	372.84
11	100	0.585	0.039	0.80	326.54	100	1.175	0.078	0.63	377.01
12	100	0.610	0.066	0.67	333.10	85	0.623	0.066	0.60	380.43
13	100	0.709	0.061	0.72	342.19	94	1.551	0.064	0.55	384.96
14	86	0.925	0.069	0.68	347.39	100	0.982	0.082	0.59	386.18
15	100	1.130	0.057	0.68	350.84	98	1.260	0.079	0.54	388.09
16	100	0.783	0.079	0.72	358.76	69	0.654	0.074	0.39	391.36
Average	98.87	0.697	0.058	0.69	321.31	93.06	0.992	0.077	0.51	354.64

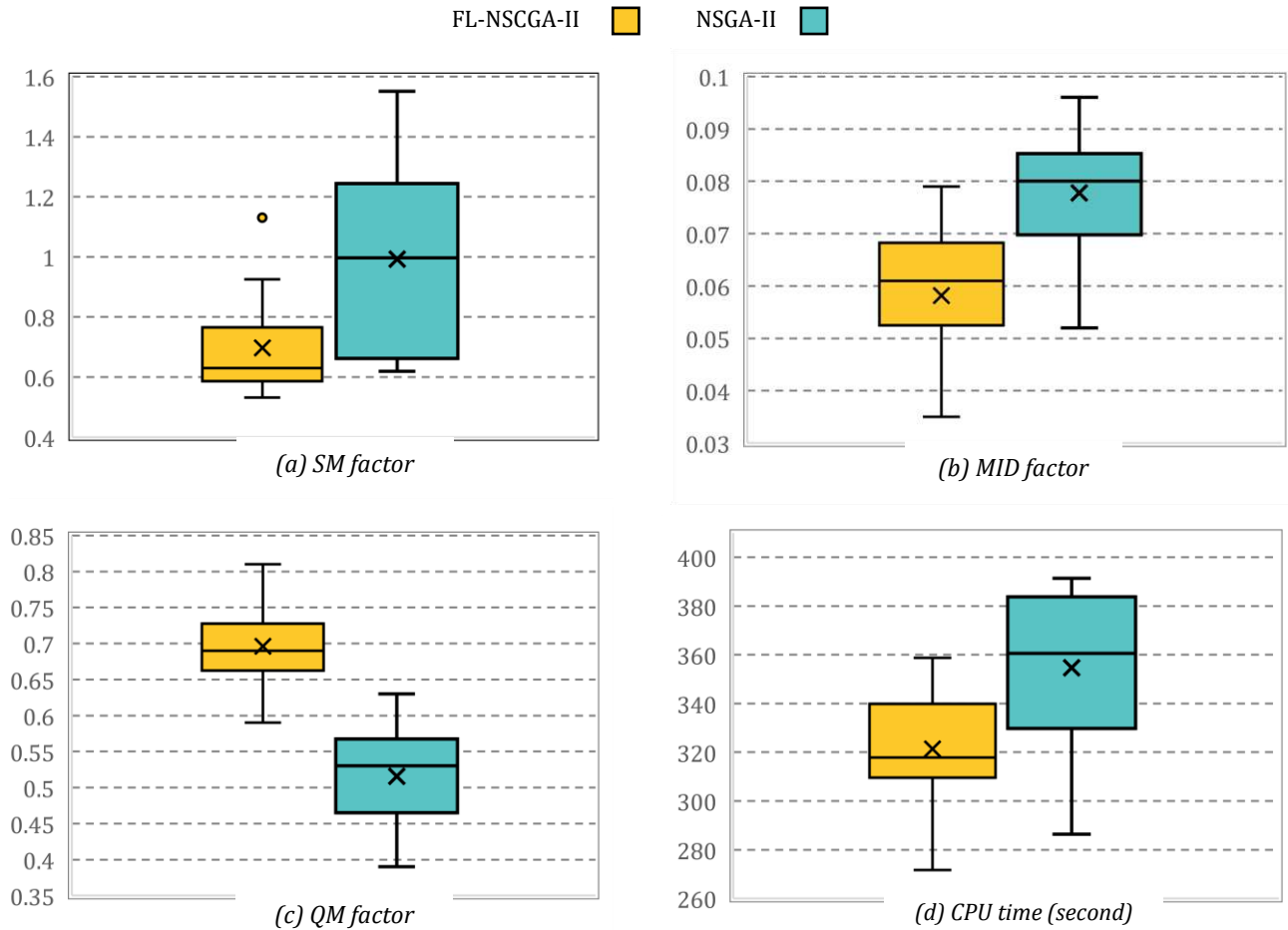


Figure 10. The performance of the FL-NSCGA-II in comparison to NSGA-II

Table 8. The P-values of the paired t-test for different metrics.

Metric's name	T-value	P-value	Test results
SM	-3.64	0.002	Null hypothesis is rejected
MID	-6.15	0	Null hypothesis is rejected
QM	9.30	0	Null hypothesis is rejected
CPU time	-10.39	0	Null hypothesis is rejected

2

6.3.2. Benefit of caching strategy and fuzzy logic guidance in FL-NSCGA-II

4

Figure 11 shows the trend of cache usage during execution with 100 iterations for instance number 9. The figure confirms that by increasing the number of iterations, the FL-NSCGA-II benefits more from the existence of internal data storage. The reason is that in the initial iterations, the algorithm encounters many undiscovered solutions that should be evaluated and stored in the cache table. Then, gradually several repetitive individuals are met in the search process and related fitness values can be evoked from the cached information. Besides, Figure 11 indicates the capability of FL-NSCGA-II to diversity the individuals of populations in comparison to pure NSGA-II. In order to figure out how the fuzzy logic guidance can separately bring diversity into the population list, the immigration procedure is discarded in FL-NSCGA-II and the obtained result is depicted in Figure 11 by the label FL-NSGA-II. This analysis shows that both added diversification techniques have a significant effect on generating dissimilar members.

12

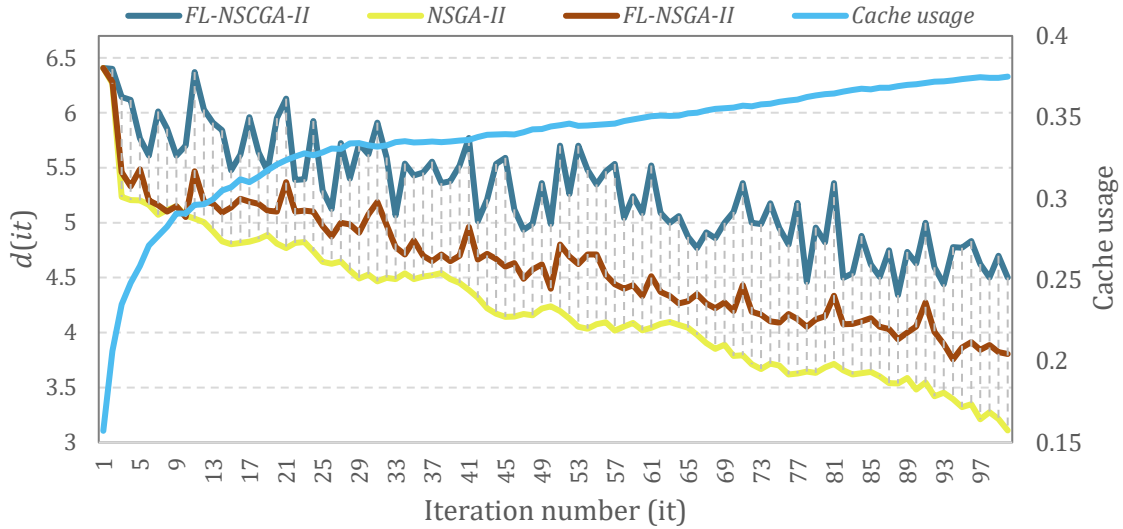


Figure 11. The benefit of caching process and FL strategy in diversification of individuals in FL-NSCGA-II

14

6.3.3. Sensitivity analysis

16

In this section, we show the sensitivity of PTDSTP-PF concerning the important parameters of the model. In the first step, we evaluate the effects of the congestion level on risk level and customer satisfaction. Five conditions are considered for the vehicle speeds by multiplying the vehicle' speeds in Table 3 to {0.5, 0.75, 1, 1.25, 1.5} which reflects the different congestion levels {Very low, Low, Normal, High, Very high} in Figure 12. In the figure, the best value for each objective function among the achieved Pareto set is reported. A glance at Figure 12 reveals traffic congestion has a significant effect on the outcomes of f_{risk} and f_s . Figure 12 indicates that an increase in the congestion levels causes an increase in the transportation risk while the total satisfaction rate decreases. The reason is that in higher traffic congestions, the travel time between each two sequential nodes increases; therefore, not only the transportation risk increases but also reaching the customers at their desired time becomes challenging. Here, two instances, eight and ten, are selected randomly for the investigations; however, all instances eventuate the same overall result.

26

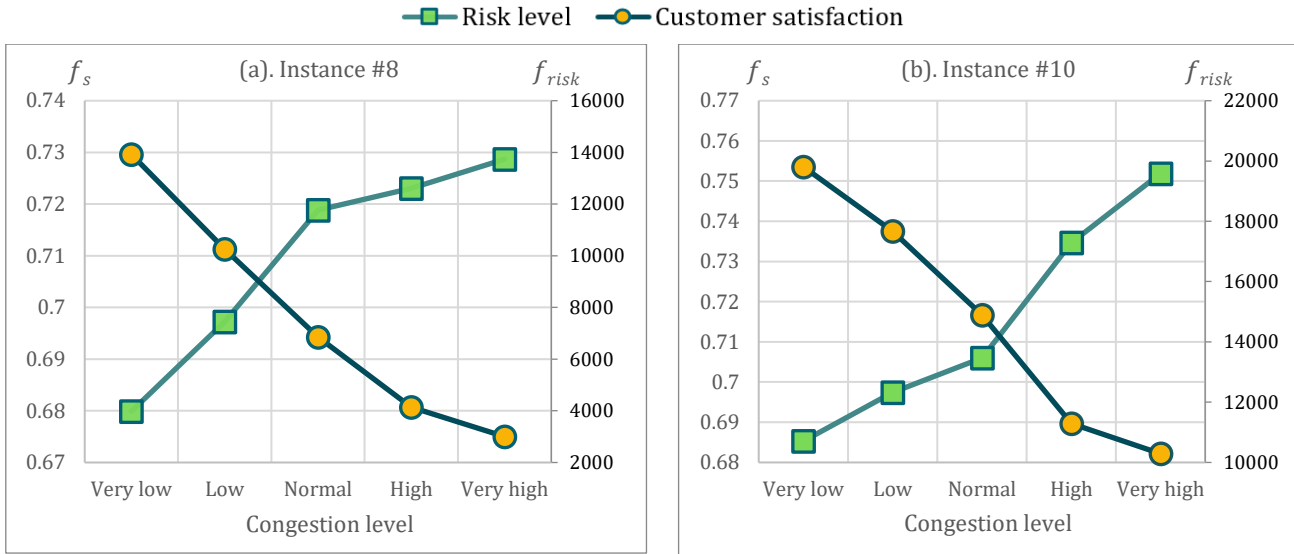


Figure 12. Effects of traffic congestion on customer satisfaction and risk level

In further analysis, the effects of risk intensity value (ψ_{ijm}) is tested on the objectives of PTDSTP-PF. As noted before, the parameter ψ_{ijm} controls the usage frequency of links in the planned routes. To do this, we investigate instance 10 with five values of ψ_{ijm} in Figure 13. In this figure, the best value according to the risk objective among the obtained Pareto set is reported. The observations show that by setting large values for ψ_{ijm} , the risk of transportation is negatively impacted and for this special solution the travel time is increased, and the customer satisfaction rate is decreased. It is apparent that by penalizing the recurrence of links in routing plans, PTDSTP-PF attempts to find dissimilar alternative routes by reordering the sequence of customers or changing the links among the vertices.

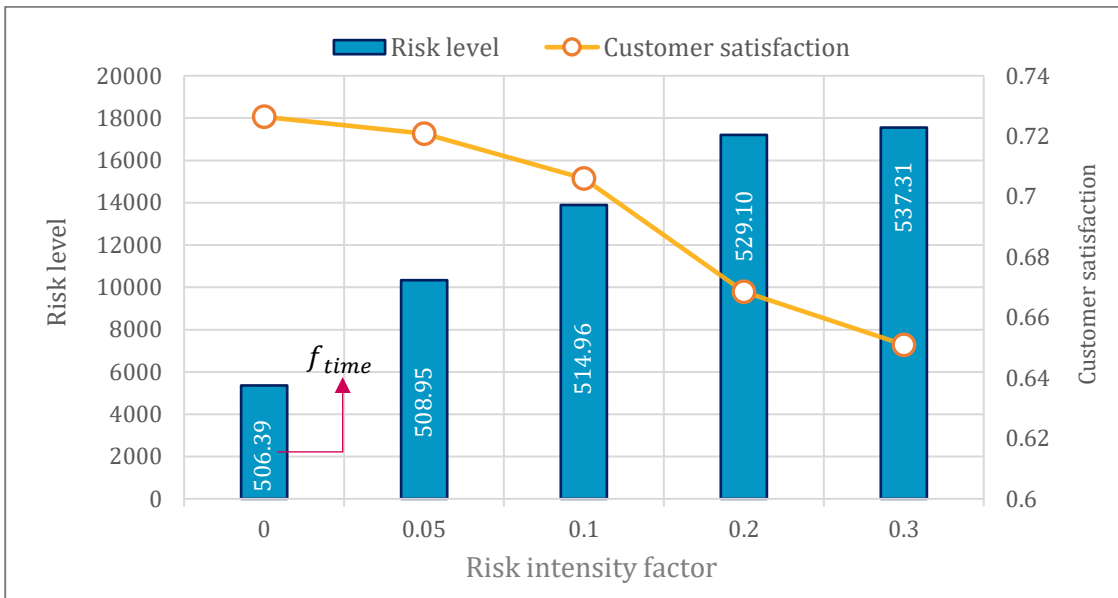


Figure 13. Effects of risk intensity value on risk of transportation for instance #10

In the following analysis, the impact of alternative paths in a multigraph structure is explored on the solution quality of the PTDSTP-PF. To transform the multigraph version into a simple graph, we randomly select one edge between each pair of nodes. Herein, the instances of Table 6 are resolved with the mentioned modification and the results are given in Table 9. The best value corresponds to each objective function among the obtained Pareto set is

reported in Table 9. Column “difference%” presents the improvements achieved by multigraph representation using equation $\frac{|OV_{SG}-OV_{MG}|}{OV_{SG}} \times 100$, where OV_{MG} and OV_{SG} indicate the objective values (OV) of multigraph and simple graph, respectively. It is evident from Table 9 that maximum and average enhancement induced by the use of multigraph structure are 12.1% and 7.28%, respectively.

Table 9. The best objective values of PTDSTP-PF in multigraph via simple graph networks

Instance	multigraph			simple graph			difference %		
	f_{time}	f_{risk}	f_s	f_{time}	f_{risk}	f_s	f_{time}	f_{risk}	f_s
3	246.84	15651.71	0.898	255.77	17325.18	0.841	3.4	9.65	6.70
7	331.36	20046.06	0.815	338.71	22671.10	0.765	2.1	11.57	6.53
10	514.96	13891.45	0.706	547.08	16628.34	0.673	5.8	16.45	4.90
14	763.97	30423.17	0.647	785.98	34081.86	0.606	2.8	10.73	6.76
Total average:							3.52	12.10	6.22

Table 9 reveals that capturing alternative links with multiple inherent attributes yields to access efficient solutions in cash transportation problems. We observe a larger difference between multigraph and simple graph for the defined transportation risk in PTDSTP-PF. The reason is that in simple graph the only way to generate dissimilar routing plans is reordering the sequence of nodes.

6.4. Managerial insights

Our findings show that the use of multigraph networks in the CIT routing problem, where both transportation risk and travel time are important, yields a significant improvement in the solution quality. Such representation not only enables CIT companies to address the tradeoffs between the attributes of links but also helps to design dissimilar routing patterns by diversifying the paths throughout the planning horizon. As mentioned, the problem is investigated under tri-objective setting and a set of non-dominated solutions is presented to a decision-maker to choose a solution that better suits the preference of customers. The following insights could be useful for practitioners:

- Proposed PTDSTP-PF model helps to increase the average satisfaction level by classifying the customers into several groups based on their importance. To do this, the demand nodes can be assigned to different predefined groups by an expert. Accordingly, a higher grade of satisfaction in a routing plan implies that most of the customers are visited before the latest desirable arrival time.
- A novel risk assessment framework is developed for PTDSTP-PF, which can consider the characteristics of available links, path diversification, arrival time variability, and asset loss exposure.
- Decision-makers can decrease the usage frequency of links in the planning horizon by setting higher values for risk intensity factor ψ_{ijm} . Moreover, the given parameters (ξ_i) can control the inconsistency of arrival times at each customer. Both adjustment parameters ψ_{ijm} and ξ_i affect the path dissimilarity in PTDSTP-PF.
- Traffic congestion in inner-city roads is another unavoidable factor in cash transportation which causes a negative effect on both customer satisfaction and risk level. Herein, PTDSTP-PF is modeled as a periodic time-dependent VRP where the travel time of each link varies according to the vehicle’s entry time. Note that in addition to the path dissimilarity’s parameters, traffic congestion of parallel links is a significant item in selecting a proper link between two sequential nodes.

7. Concluding remarks

This paper presents a novel mathematical model for a periodic time-dependent secure transportation problem with path flexibility by satisfying the FIFO consistency, named as PTDSTP-PF. In terms of mathematical formulation, this is the first study that focused on the benefits of path flexibility and its importance in designing safe and dissimilar routing plans over different periods. PTDSTP-PF includes a comprehensive risk assessment framework to consider

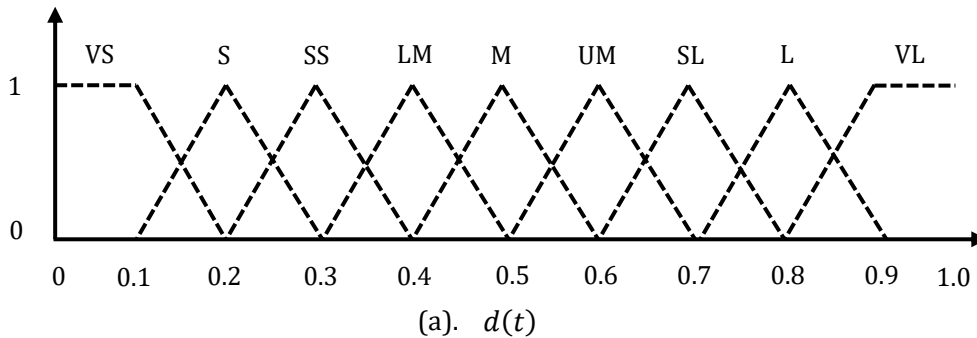
the path diversification, arrival time variability, asset loss exposure, time-varying traffic congestions, etc. The path diversification mechanism increases security by penalizing the use of repetitive links over the planning horizon. And since the problem is studied in a multigraph setting, alternative solutions can be constructed not only by reordering the sequence of nodes but also by exchanging the available links among the vertices in a multigraph network. Moreover, the arrival time variability imposes a pre-specified time constant for consecutive visits at the same demand node.

The PTDSTP-PF has been interpreted as a multi-objective routing problem, in which the total required completion times and transportation risks are minimized and the customers' satisfaction level is maximized. In the latter objective, customers are segmented according to their preferences; then specific time windows are considered for each class of customers to reflect the level of satisfaction. From a methodological view, it is hard to solve the PTDSTP-PF due to its challenging features such as time-dependency, nonlinearity, multi-period planning, and multigraph representation. Herein, we proposed a novel NSGA-II coupled with some innovative techniques such as caching mechanism and fuzzy logic approach, which can dynamically adjust the rates of operators during the searching process. To evaluate the overall performance of the FL-NSCGA-II algorithm, we compared it with standard NSGA-II.

Comparisons on performance metrics show that proposed FL-NSCGA-II stands out as a more effective method. The performed statistical test also confirmed this superiority. In further analysis, we analyzed the sensitivity of the model's input parameters and in particular the efficiency of using multigraph network. The results imply that such representation yields to access efficient solutions in the proposed cash transportation problem. More specifically, we observed a significant improvement in the transportation risk of multigraph versus simple graph. The reason is that a multigraph network is more applicable in construction of dissimilar routing plans since it can keep more than one arc among nodes. The possible directions envisaged for future works include addressing the stochastic version of PTDSTP-PF and considering different cash denominations demanded by the customers.

Appendix A. Fuzzy logic process

Fuzzification: In any fuzzy logic process, it is necessary to define membership functions associated with the input/output values. In this regard, we adopted triangular membership functions (based on Lau et al., 2009) where the system includes two inputs $f_a(it) - f_a(it - 9)$ and $d(it)$. Figures A.1 presents the membership functions for two fuzzy controllers and Figures A.2 depicts the membership functions of system outputs. The meaning of each linguistic term is also listed in Tables A.1- A.2.



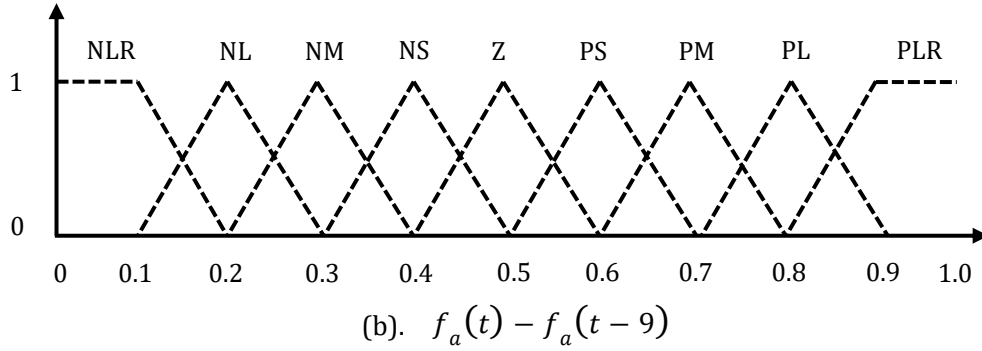


Figure A.1. Membership functions of inputs $f_a(t) - f_a(t - 9)$ and $d(t)$

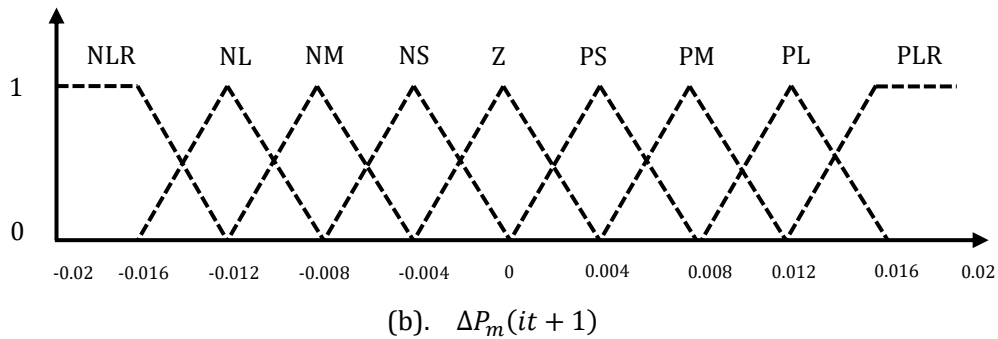
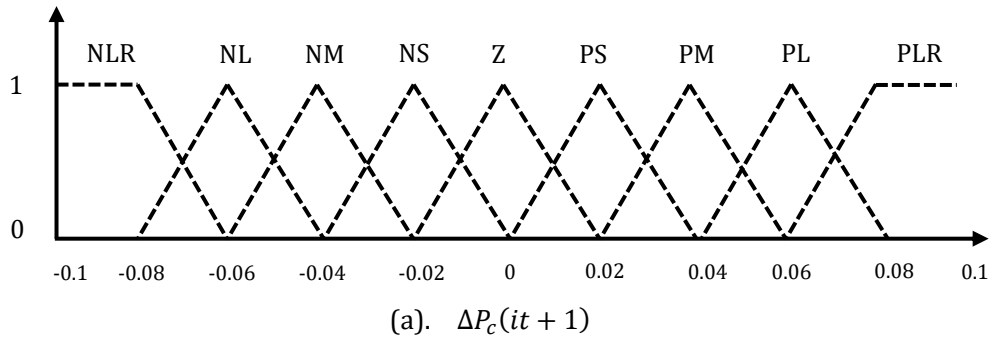


Figure A.2. Membership functions for change of crossover/mutation rates

Table A.1. Meaning of each linguistic term in Figure A.1 (a).

Terms	Meaning
VS	Very small
S	Small
SS	Slightly small
LM	Lower medium
M	Medium
UM	Upper medium
SL	Slightly large
L	Large
VL	Very large

Table A.2. Meaning of each linguistic term in Figure A.1 (b) and Figure A.2.

Terms	Meaning
NLR	Negative larger
NL	Negative large
NM	Negative medium
NS	Negative small
Z	Zero
PS	Positive small
PM	Positive medium
PL	Positive large
PLR	Positive larger

Fuzzy rules: Fuzzy rules must be defined within our fuzzy logic guided systems to infer outputs based on input membership variables. These rules, which are tabulated in Table A.3, are presented according to Lau et al. (2009) and based on consultation with professional experts. The sets of defined rules for output membership values of $\Delta P_c(it + 1)$ and $\Delta P_m(it + 1)$ are given in Table A.3 and Table A.4, respectively. An example of the defined IF/THEN rule is as follows:

IF $d(it)$ is VL, **AND** $f_a(it) - f_a(it - 9)$ is PLR **THEN** output is Z.

Table A.3. The defined set of IF-THEN rules for $\Delta P_c(it + 1)$

	NLR	NL	NM	NS	Z	PS	PM	PL	PLR
VS	Z	NS	NS	NM	NM	NL	NL	NLR	NLR
S	PS	Z	NS	NS	NM	NM	NL	NL	NLR
SS	PS	PS	Z	NS	NS	NM	NM	NL	NL
LM	PM	PS	PS	Z	NS	NS	NM	NM	NL
M	PM	PM	PS	PS	Z	NS	NS	NM	NM
UM	PL	PM	PM	PS	PS	Z	NS	NS	NM
SL	PL	PL	PM	PM	PS	PS	Z	NS	NS
L	PLR	PL	PL	PM	PM	PS	PS	Z	NS
VL	PLR	PLR	PL	PL	PM	PM	PS	PS	Z

Table A.4. The defined set of IF-THEN rules for $\Delta P_m(it + 1)$

	NLR	NL	NM	NS	Z	PS	PM	PL	PLR
VS	Z	PS	PS	PM	PM	PL	PL	PLR	PLR
S	NS	Z	PS	PS	PM	PM	PL	PL	PLR
SS	NS	NS	Z	PS	PS	PM	PM	PL	PL
LM	NM	NS	NS	Z	PS	PS	PM	PM	PL
M	NM	NM	NS	NS	Z	PS	PS	PM	PM
UM	NL	NM	NM	NS	NS	Z	PS	PS	PM
SL	NL	NL	NM	NM	NS	NS	Z	PS	PS
L	NLR	NL	NL	NM	NM	NS	NS	Z	PS
VL	NLR	NLR	NL	NL	NM	NM	NS	NS	Z

Defuzzification: This module is used to present a crisp value according to the fuzzy inference results. Among several exited forms of defuzzification procedures, we applied the center of area referred to *centroid* as one of the most common approaches in the literature. This method considers the center of area of fuzzy set to give the corresponding crisp output. For further information about this approach, we refer the reader to Wang (2001).

Acknowledgements:

We thank reviewers for their helpful suggestions and comments. Overall, the research and manuscript have benefitted from the resulting changes.

References:

- Alinaghian, M., & Naderipour, M. (2016). A novel comprehensive macroscopic model for time-dependent vehicle routing problem with multi-alternative graph to reduce fuel consumption: A case study. *Computers & Industrial Engineering*, 99, 210-222.
- Androutsopoulos, K. N., & Zografos, K. G. (2017). An integrated modelling approach for the bicriterion vehicle routing and scheduling problem with environmental considerations. *Transportation Research Part C: Emerging Technologies*, 82, 180-209.
- Archetti, C., Fernández, E., & Huerta-Muñoz, D. L. (2017). The flexible periodic vehicle routing problem. *Computers & Operations Research*, 85, 58-70.

2 Basso, R., Kulcsár, B., Egardt, B., Lindroth, P., & Sanchez-Diaz, I. (2019). Energy consumption estimation integrated into the electric
vehicle routing problem. *Transportation Research Part D: Transport and Environment*, 69, 141-167.

4 Behnke, M., & Kirschstein, T. (2017). The impact of path selection on GHG emissions in city logistics. *Transportation Research Part E:
Logistics and Transportation Review*, 106, 320-336.

6 Behnke, M., Kirschstein, T., & Bierwirth, C. (2020). A column generation approach for an emission-oriented vehicle routing problem
on a multigraph. *European Journal of Operational Research*.

8 Beltrami, E. J., & Bodin, L. D. (1974). Networks and vehicle routing for municipal waste collection. *Networks*, 4(1), 65-94.

10 Bozkaya, B., Salman, F. S., & Telciler, K. (2017). An adaptive and diversified vehicle routing approach to reducing the security risk of
cash-in-transit operations. *Networks*, 69(3), 256-269.

12 Bruglieri, M., Mancini, S., Pezzella, F., & Pisacane, O. (2019). A path-based solution approach for the green vehicle routing
problem. *Computers & Operations Research*, 103, 109-122.

14 Cacchiani, V., Hemmelmayr, V. C., & Tricoire, F. (2014). A set-covering based heuristic algorithm for the periodic vehicle routing
problem. *Discrete Applied Mathematics*, 163, 53-64.

16 Calvo, R. W., & Cordone, R. (2003). A heuristic approach to the overnight security service problem. *Computers & Operations
Research*, 30(9), 1269-1287.

18 Campbell, A. M., & Wilson, J. H. (2014). Forty years of periodic vehicle routing. *Networks*, 63(1), 2-15.

20 Capgemini Research Institute. World Payments Report 2019. Accessed August 2020. [https://www.capgemini.com/es-es/wp-
content/uploads/sites/16/2019/09/World-Payments-Report-WPR-2019.pdf](https://www.capgemini.com/es-es/wp-content/uploads/sites/16/2019/09/World-Payments-Report-WPR-2019.pdf)

22 Chen, R. M., Shen, Y. M., & Hong, W. Z. (2019). Neural-like encoding particle swarm optimization for periodic vehicle routing
problems. *Expert Systems with Applications*, 138, 112833.

24 Constantino, M., Mourão, M. C., & Pinto, L. S. (2017). Dissimilar arc routing problems. *Networks*, 70(3), 233-245.

26 Dayarian, I., Crainic, T. G., Gendreau, M., & Rei, W. (2015). A branch-and-price approach for a multi-period vehicle routing
problem. *Computers & Operations Research*, 55, 167-184.

28 Deb, K., Pratap, A., Agarwal, S., & Meyarivan, T. A. M. T. (2002). A fast and elitist multiobjective genetic algorithm: NSGA-II. *IEEE
transactions on evolutionary computation*, 6(2), 182-197.

30 Ehmke, J. F., Campbell, A. M., & Thomas, B. W. (2018). Optimizing for total costs in vehicle routing in urban areas. *Transportation
Research Part E: Logistics and Transportation Review*, 116, 242-265.

32 Fallah-tafti, A., Vahdatzad, M. A., & Sadeghieh, A. (2019). A Comprehensive Mathematical Model for a Location-routing-inventory
Problem under Uncertain Demand: a Numerical Illustration in Cash-in-transit Sector. *International Journal of Engineering*, 32(11), 1634-
1642.

34 Federal Reserve. 2020. Findings from the Diary of Consumer Payment Choice. Accessed August 2020. <https://www.frbsf.org/cash/publications/fed-notes/2020/july/2020-findings-from-the-diary-of-consumer-payment-choice/>.

36 Francis, P. M., Smilowitz, K. R., & Tzur, M. (2008). The period vehicle routing problem and its extensions. In *The vehicle routing problem:
latest advances and new challenges* (pp. 73-102). Springer, Boston, MA.

38 Garaix, T., Artigues, C., Feillet, D., & Josselin, D. (2010). Vehicle routing problems with alternative paths: An application to on-demand
transportation. *European Journal of Operational Research*, 204(1), 62-75.

40 Geismar, H. N., Sriskandarajah, C., & Zhu, Y. (2017). A review of operational issues in managing physical currency supply
chains. *Production and Operations Management*, 26(6), 976-996.

42 Ghannadpour, S. F., & Zandiyeh, F. (2020). A new game-theoretical multi-objective evolutionary approach for cash-in-transit vehicle
routing problem with time windows (A Real life Case). *Applied Soft Computing*, 106378.

44 Ghannadpour, S. F., & Zarrabi, A. (2019). Multi-objective heterogeneous vehicle routing and scheduling problem with energy
minimizing. *Swarm and evolutionary computation*, 44, 728-747.

46 Gmira, M., Gendreau, M., Lodi, A., & Potvin, J. Y. (2020). Tabu Search for the Time-Dependent Vehicle Routing Problem with Time
Windows on a Road Network. *European Journal of Operational Research*.

48 Hiermann, G., Hartl, R. F., Puchinger, J., & Vidal, T. (2019). Routing a mix of conventional, plug-in hybrid, and electric vehicles. *European
Journal of Operational Research*, 272(1), 235-248.

Hoogeboom, M., & Dullaert, W. (2019). Vehicle routing with arrival time diversification. *European Journal of Operational
Research*, 275(1), 93-107.

2 Hu, H., Li, X., Zhang, Y., Shang, C., & Zhang, S. (2019). Multi-objective location-routing model for hazardous material logistics with traffic
restriction constraint in inter-city roads. *Computers & Industrial Engineering*, 128, 861-876.

4 Huang, Y., Zhao, L., Van Woensel, T., & Gross, J. P. (2017). Time-dependent vehicle routing problem with path flexibility. *Transportation
Research Part B: Methodological*, 95, 169-195.

6 Ichoua, S., Gendreau, M., & Potvin, J. Y. (2003). Vehicle dispatching with time-dependent travel times. *European journal of operational
research*, 144(2), 379-396.

8 Koç, Ç, Bektaş, T., Jabali, O., & Laporte, G. (2016). The impact of depot location, fleet composition and routing on emissions in city
logistics. *Transportation Research Part B: Methodological*, 84, 81-102.

10 Kuo, Y. (2010). Using simulated annealing to minimize fuel consumption for the time-dependent vehicle routing problem. *Computers
& Industrial Engineering*, 59(1), 157-165.

12 Lai, D. S., Demirag, O. C., & Leung, J. M. (2016). A tabu search heuristic for the heterogeneous vehicle routing problem on a
multigraph. *Transportation Research Part E: Logistics and Transportation Review*, 86, 32-52.

14 Larrain, H., Coelho, L. C., & Cataldo, A. (2017). A variable MIP neighborhood descent algorithm for managing inventory and distribution
of cash in automated teller machines. *Computers & Operations Research*, 85, 22-31.

16 Lau, H. C., Chan, T. M., Tsui, W. T., Chan, F. T., Ho, G. T., & Choy, K. L. (2009). A fuzzy guided multi-objective evolutionary algorithm model
for solving transportation problem. *Expert Systems with Applications*, 36(4), 8255-8268.

18 Lotfi, A. A., & Kashani, F. H. (2004, June). Bandwidth optimization of the E-shaped microstrip antenna using the genetic algorithm based
on fuzzy decision making. In *IEEE Antennas and Propagation Society Symposium, 2004*. (Vol. 3, pp. 2333-2336). IEEE.

20 Luo, Z., Qin, H., Che, C., & Lim, A. (2015). On service consistency in multi-period vehicle routing. *European Journal of Operational
Research*, 243(3), 731-744.

22 Martí, R., Velarde, J. L. G., & Duarte, A. (2009). Heuristics for the bi-objective path dissimilarity problem. *Computers & Operations
Research*, 36(11), 2905-2912.

24 Michallet, J., Prins, C., Amodeo, L., Yalaoui, F., & Vitry, G. (2014). Multi-start iterated local search for the periodic vehicle routing problem
with time windows and time spread constraints on services. *Computers & operations research*, 41, 196-207.

26 Nemati-Lafmejani, R., Davari-Ardakani, H., & Najafzad, H. (2019). Multi-mode resource constrained project scheduling and contractor
selection: Mathematical formulation and metaheuristic algorithms. *Applied Soft Computing*, 81, 105533.

28 Ngueveu, S. U., Prins, C., & Calvo, R. W. (2010). Lower and upper bounds for the m-peripatetic vehicle routing problem. *4OR*, 8(4), 387-
406.

30 Radojičić, Nina, Aleksandar Djenić, and Miroslav Marić. "Fuzzy GRASP with path relinking for the Risk-constrained Cash-in-Transit
Vehicle Routing Problem." *Applied Soft Computing* 72 (2018): 486-497.

32 Radojičić, Nina, Miroslav Marić, and Aleksandar Takači. "A New Fuzzy Version of the Risk-constrained Cash-in-Transit Vehicle Routing
Problem." *Information Technology and Control* 47.2 (2018): 321-337.

34 Raeesi, R., & Zografos, K. G. (2019). The multi-objective Steiner pollution-routing problem on congested urban road
networks. *Transportation Research Part B: Methodological*, 122, 457-485.

36 Rayat, F., Musavi, M., & Bozorgi-Amiri, A. (2017). Bi-objective reliable location-inventory-routing problem with partial backordering
under disruption risks: A modified AMOSA approach. *Applied Soft Computing*, 59, 622-643.

38 Reinhardt, L. B., Jepsen, M. K., & Pisinger, D. (2015). The edge set cost of the vehicle routing problem with time windows. *Transportation
Science*, 50(2), 694-707.

40 Repolho, H. M., Marchesi, J. F., Júnior, O. S. S., & Bezerra, R. R. (2019). Cargo theft weighted vehicle routing problem: modeling and
application to the pharmaceutical distribution sector. *Soft Computing*, 23(14), 5865-5882.

42 Setak, M., Habibi, M., Karimi, H., & Abedzadeh, M. (2015). A time-dependent vehicle routing problem in multigraph with FIFO
property. *Journal of Manufacturing Systems*, 35, 37-45.

44 Setak, M., Z. Shakeri, and A. Patoghi. (2017). A time dependent pollution routing problem in multi-graph. *International Journal of
Engineering*, 30(2), 234-242.

46 Soriano, A., Vidal, T., Gansterer, M., & Doerner, K. (2020). The vehicle routing problem with arrival time diversification on a
multigraph. *European Journal of Operational Research*.

48 Talarico, L. (2016). *Secure vehicle routing: models and algorithms to increase security and reduce costs in the cash-in-transit
sector* (Doctoral dissertation, Springer Berlin Heidelberg).

2 Talarico, L., Sörensen, K., & Springael, J. (2013). The risk-constrained cash-in-transit vehicle routing problem with time window
constraints. In *14th Workshop of the EURO Working Group* (pp. 104-109).

4 Talarico, L., Sörensen, K., & Springael, J. (2015a). Metaheuristics for the risk-constrained cash-in-transit vehicle routing
problem. *European Journal of Operational Research*, *244*(2), 457-470.

6 Talarico, L., Sörensen, K., & Springael, J. (2015b). The k-dissimilar vehicle routing problem. *European Journal of Operational
Research*, *244*(1), 129-140.

8 Talarico, L., Sörensen, K., & Springael, J. (2017a). A biobjective decision model to increase security and reduce travel costs in the cash-
in-transit sector. *International Transactions in Operational Research*, *24*(1-2), 59-76.

10 Talarico, L., Springael, J., Sörensen, K., & Talarico, F. (2017b). A large neighbourhood metaheuristic for the risk-constrained cash-in-
transit vehicle routing problem. *Computers & Operations Research*, *78*, 547-556.

12 Ticha, H. B., Absi, N., Feillet, D., & Quilliot, A. (2017). Empirical analysis for the VRPTW with a multigraph representation for the road
network. *Computers & Operations Research*, *88*, 103-116.

14 Ticha, H. B., Absi, N., Feillet, D., & Quilliot, A. (2019). Multigraph modeling and adaptive large neighborhood search for the vehicle
routing problem with time windows. *Computers & Operations Research*, *104*, 113-126.

16 Tikani, H., & Setak, M. (2019). Efficient solution algorithms for a time-critical reliable transportation problem in multigraph networks
with FIFO property. *Applied Soft Computing*, *74*, 504-528.

18 Van Anholt, R. G., Coelho, L. C., Laporte, G., & Vis, I. F. (2016). An inventory-routing problem with pickups and deliveries arising in the
replenishment of automated teller machines. *Transportation Science*, *50*(3), 1077-1091.

20 Wang, H., Du, L., & Ma, S. (2014). Multi-objective open location-routing model with split delivery for optimized relief distribution in
post-earthquake. *Transportation Research Part E: Logistics and Transportation Review*, *69*, 160-179.

22 Wang, K. (2001). Computational intelligence in agile manufacturing engineering. *Agile Manufacturing The 21st Century Competitive
Strategy*, Oxford, UK: Elsevier Science Ltd, 297-315.

24 Xu, G., Li, Y., Szeto, W. Y., & Li, J. (2019). A cash transportation vehicle routing problem with combinations of different cash
denominations. *International Transactions in Operational Research*, *26*(6), 2179-2198.

26 Yan, S., Wang, S. S., & Wu, M. W. (2012). A model with a solution algorithm for the cash transportation vehicle routing and scheduling
problem. *Computers & Industrial Engineering*, *63*(2), 464-473.

28 Zajac, S. (2016). The bi-objective k-dissimilar vehicle routing problem. In *International Conference on Computational Logistics* (pp. 306-
320). Springer, Cham.

30 Zajac, S. (2018). On a two-phase solution approach for the bi-objective k-dissimilar vehicle routing problem. *Journal of Heuristics*, *24*(3),
515-550.